Food Hydrocolloids 149 (2024) 109519

Contents lists available at ScienceDirect

Food Hydrocolloids

journal homepage: www.elsevier.com/locate/foodhyd

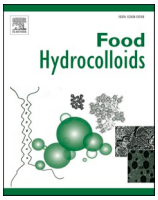

Stabilising and functional effects of Spirulina (*Arthrospira platensis*) protein isolate on encapsulated *Lacticaseibacillus rhamnosus* GG during processing, storage and gastrointestinal digestion

Jennyfer Fortuin [a,b], Thierry Hellebois [a], Marcus Iken [c], Alexander S. Shaplov [d], Vincenzo Fogliano [b], Christos Soukoulis [a,*]

[a] *Environmental Research and Innovation (ERIN) Department, Luxembourg Institute of Science and Technology (LIST), 5 Avenue des Hauts Fourneaux, L4362, Esch-sur-Alzette, Luxembourg*
[b] *Food Quality and Design Group, Wageningen University and Research, 6708 NL, Wageningen, the Netherlands*
[c] *PM-International AG, Schengen, Luxembourg*
[d] *Materials Research and Technology (MRT) Department, Luxembourg Institute of Science and Technology (LIST), 5 Avenue des Hauts Fourneaux, L4362, Esch-sur-Alzette, Luxembourg*

ARTICLE INFO

Keywords:
Microalgae
Protein isolate
Probiotics
Encapsulation
Viability
In vitro digestion

ABSTRACT

The present study investigated Spirulina (*Arthrospira platensis*) protein isolate (SPI) for its ability to preserve the biological activity of *L. rhamnosus* GG (LGG) cells under diverse physicochemical stressors associated with the lyophilisation process, storage, and *in vitro* digestion. The lyoprotective and stabilising effects of SPI were compared to whey protein isolate (WPI) and pea protein isolate (PPI). The microstructural, physicochemical, and thermal properties of the probiotic lyophilisates were also assessed. Overall, SPI demonstrated superior lyoprotective and storage stabilising effects compared to WPI, although it was less efficient than PPI. Elevated storage temperature and relative humidity (RH) conditions accelerated LGG inactivation rates, especially in the case of WPI, which was primarily attributed to increased LGG's metabolic activity. The fermentation of the probiotic freeze-drying media impaired LGG's ability to withstand the physicochemical stressors during lyophilization and storage. However, the pre-fermentation step improved LGG's resistance to harsh acidic conditions in simulated gastric fluids. Bile salts and pancreases did not significantly affect LGG's survivability, with WPI and PPI showing the most effectiveness. Employing an *in vitro* co-culture model of the gut epithelium, WPI and PPI demonstrated satisfactory adhesion of LGG cells to the mucus layer, displaying the highest cell adhesion potential. In conclusion, SPI appears to be a promising wall material for probiotic cell encapsulation, serving as an alternative to WPI.

1. Introduction

Over the past two decades, consumer awareness has steadily increased regarding the link between dietary habits, lifestyle choices, and the onset of chronic health complications, such as type-II diabetes, cardiovascular disease, obesity, and various forms of cancer. This has raised the interest of the food and nutraceutical industry stakeholders in the identification of new ingredients that exert a multi-faceted technological and bio-functional profile. Microalgae constitute a group of morphologically and physiologically diversified unicellular, oxygen-evolving, photosynthetic microorganisms found in aquatic environments (Grossmann et al., 2020). Microalgal biomass is a rapidly expanding bioresource and is composed of macro- and micro-constituents relevant to food, including food biopolymers (e.g., polysaccharides, proteins, and lipids) and bioactive secondary metabolites (e.g., vitamins, carotenoids, phycobiliproteins, polyphenols, chlorophylls, etc.) (Buono et al., 2014; Caporgno & Mathys, 2018; Grossmann et al., 2020). It is characteristic that forecasts on the microalgal ingredients market indicate an expansion from $977 M in 2020 to $1487 M in 2028 (Frost & Sullivan, 2023).

Spirulina is the commercial name of two species of planktonic photosynthetic cyanobacteria, namely *Arthrospira platensis* and *Arthrospira maxima* (Soni et al., 2017). Spirulina is one of the richest microalgal biomass sources, with its protein content ranging from 60 to 70%

* Corresponding author.
E-mail address: christos.soukoulis@list.lu (C. Soukoulis).

https://doi.org/10.1016/j.foodhyd.2023.109519
Received 22 September 2023; Received in revised form 27 October 2023; Accepted 6 November 2023
Available online 13 November 2023

depending on the life stage, cultivation conditions and the methodologies implemented for the extraction, isolation and drying (Moreira et al., 2023). In addition, spirulina proteins have a well-balanced essential amino acids composition, and they are well digestible (up to 80%). Apart from their high biological value, Spirulina proteins have good techno-functional properties. They have been successfully employed in the structuring, stabilising and texturing of processed novel foods due to their multifaceted techno-functionality such as good water solubility (up to 67%) (Chen et al., 2019), high interfacial activity (Bertsch et al., 2021), good water and oil holding capacity (Boukhari et al., 2018), as well as fair gelation (Shkolnikov Lozober et al., 2021) and film forming capacity (Benelhadj et al., 2016). Hitherto, the technological relevance of spirulina to the functional food industry has been showcased in cereal-based products such as pasta, bread and biscuits, extruded snacks, fermented dairy products such as yoghurt and cheese, meat analogues, vegetable-based preparations, etc. (Lafarga et al., 2020). Additionally, the use of raw spirulina biomass or its bioactive fractions in the production of food supplements imparting several health conferring benefits, including prebiotic effects, immunostimulatory, anti-inflammatory and antitumor activity, neuroprotective effects, and alleviation of the metabolism disorders, is well established (Bortolini et al., 2022).

The term probiotics is used to define human gut relevant commensal and microbes consortia having generic or core effects on gut physiology and homeostasis or supporting the health of the reproductive tract, oral cavity, lungs, skin and gut-brain axis (Hill et al., 2014). Although probiotics are naturally present in many fermented foods such as yoghurt, cheese, kefir, sauerkraut, kimchi, natto etc. (Şanlier et al., 2019), the fortification of processed food and nutraceutical formulations is an alternative way to administer a sufficient amount of living probiotic cells via the oral route (Kiepś & Dembczyński, 2022). In the latter case, encapsulation, i.e., the physical engrafting of labile bioactives (including living cells) in a structurally and/or interfacially engineered colloidal micro- or nano-template, is a very efficient technological approach to preserve the inherent biological activity of probiotics (Gu et al., 2022; Kiepś & Dembczyński, 2022; Yao et al., 2020). An efficient encapsulation system for probiotics should allow satisfactory protection against common physicochemical stressors encountered during processing and storage, such as heat, pH, water vapour, oxygen, osmotic stress, mechanical injuries, etc. (Capozzi et al., 2016; Gu et al., 2022; Yao et al., 2020). In addition, it should be easily programmable to minimise the cells' sublethality during gastrointestinal transit and provide sustained matrix disintegration, controlled release of the probiotic cells, and good cell adhesion to the gut mucosal tissue (Dos Santos Morais et al., 2022; Garcia-Brand et al., 2022; Gu et al., 2022; Seifert et al., 2019). Anhydrobiotic technology, i.e., the production of xero-carriers embedding living cells produced via lyophilisation or spray-drying, is considered as the commonest strategy for probiotics encapsulation (Aschenbrenner et al., 2015; Burgain et al., 2015). In view of composition, probiotic xero-carriers comprise at least one structuring thermoplastic biopolymer (e.g., starch, gums, proteins, etc.) and a lyo- or thermo-protective agent (e.g., sugars, polyols, maltodextrins) (Broeckx et al., 2017; Schwab et al., 2007). On many occasions, the incorporation of probiotic cell growth-promoting agents, i.e., prebiotics, such as inulin, galacto-oligosaccharides, fructo-oligosaccharides etc., can confer a significant preventive role against probiotics sub-lethality due to extrinsic stressors (Capela et al., 2006).

Recent studies have pinpointed the Lactobacilli and Bifidobacteria growth-promoting role of *Arthrospira platensis* biomass and its extracellular microalgal extracts (Meireles Mafaldo et al., 2022; Ricós-Muñoz et al., 2023). Ricós-Muñoz et al. (2023) demonstrated that the supplementation of modified MRS substrate with Spirulina extracts resulted in a significant stimulation of the growth of *L. rhamnosus* GG favouring the production of exopolysaccharides (EPS) and short chain free fatty acids (SCFAs) such as acetate, propionate, and butyrate under anaerobiosis for 72 h, an effect that was attributed to the presence of non-digestible oligosaccharides (NDOs).

The present study focused on the use of Spirulina (*Arthrospira platensis*) protein isolate (SPI) in lyophilisates engrafting living *Lacticaseibacillus rhamnosus* GG (LGG) cells. The research explored various methods of structuring the xero-carrier precursors, specifically, through a solution or hydrogel prepared via indirect acidification (lactic acid fermentation). The resulting xero-carriers were characterised both structurally and physicochemically, and the viability of LGG cells during freeze-drying, controlled storage, and *in vitro* gastrointestinal digestion. Moreover, the ability of the carriers to promote the adhesion of LGG cells onto the mucosa layer of co-culture model of the gut epithelium was tested. Whey protein and pea protein isolate-based xero-carrier analogues were also prepared to serve as benchmarks.

2. Materials and methods

2.1. Materials

Spirulina biomass was purchased from Sevenhills Wholefoods (Sheffield, United Kingdom). Pea protein isolate (PPI, NATURALYS S85 plus N) with a protein content of 85% wt. and whey protein isolate (WPI, PRODIET 90 S) with a protein content of 85.8% wt. were kindly donated by Roquette (Lestrem, France) and Ingredia (Arras, France), respectively. D-glucose and trehalose were purchased from Sigma-Aldrich (Leuven, Belgium) and Louis-François (Croissy-Beaubourg, France), respectively. Maltodextrin (Maltosweet 150, 15 DE, Tate & Lyle S.A.) was purchased from Elton SA (Athens, Greece). De Man, Rogosa, and Sharpe (MRS) precast plates and MRS culture media were purchased from Thermo Scientific Oxoid (Merelbeke, Belgium) and Carl Roth (Karlsruhe, Germany), respectively. *Lacticaseibacillus rhamnosus* GG (LGG) ATCC 53103 was procured from VTT Technical Research Centre of Finland Ltd (Espoo, Finland), while all other chemicals were of analytical grade and were purchased from Sigma-Aldrich (Leuven, Belgium).

2.2. Preparation of the Spirulina protein isolate

Spirulina protein isolate (SPI) was prepared according to the procedure outlined in Fig. 1. In brief, Spirulina biomass powder was dispersed in MilliQ water (18.2 mΩ, Millipore Inc., United States) at ambient temperature to achieve 10% wt. total solids. The pH of the microalgal suspension was then adjusted to pH = 7 using NaOH 5 M and kept under magnetic stirring for 2 h at room temperature. To increase the extraction yield, the suspension was homogenized 8 times at 1200 bar (Panda plus 2000, Gea, Germany). Afterwards, the pH was re-adjusted to pH 7 with NaOH 5 M.

For the separation of the soluble protein-rich supernatant from the insoluble biomass, the homogenized suspension was centrifuged for 1 h at 11,000 rpm and 20 °C (Multifuge X3R, Fiberlite F14–6, ThermoFisher, Belgium). The supernatant was then dialyzed against MilliQ water using a 12 kDa cut-off dialysis membrane (SpectraPor 4 Dialysis Membrane, Standard RC Tubing, width flat: 75 mm, Ø 48 mm) for 72 h at room temperature to remove the salts used for pH adjustment. The MilliQ water was changed every morning and evening during the dialysis process. The dialysed SPI solutions were frozen at −80 °C and then lyophilised for 7 days (Alpha 1-2LD Plus, Christ, Germany) in a freeze-dryer chamber protected from direct light.

2.3. Proximate composition of the protein isolates

Ash and moisture content were gravimetrically determined according to the AOAC standard method. The carbohydrate content was determined based on the sulfuric-acid-UV method (Albalasmeh et al., 2013). Briefly, 3 mL of concentrated sulfuric acid was added to 1 mL of 0.1% wt. SPI and vortexed for 30 s. The samples were then stored on ice to cool down before further use. An aliquot of 200 μL was added into a UV 96-well microplate (UV-Star, Greiner, Frickenhausen, Germany),

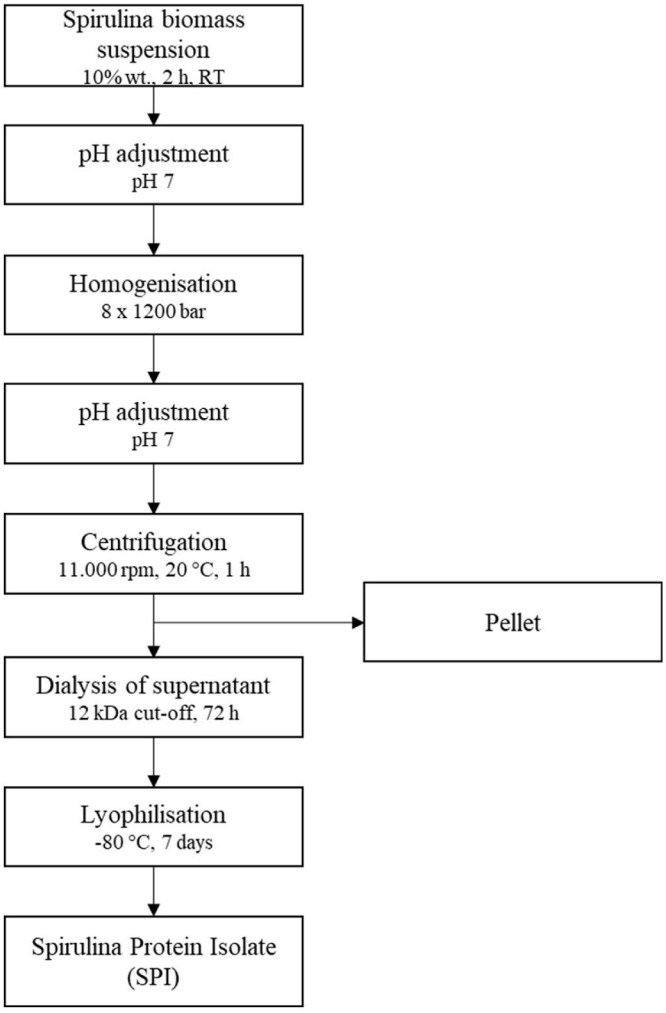

Fig. 1. Illustration of the procedure implemented for the preparation of Spirulina protein isolates.

and the absorbance at 315 nm was measured using a UV/VIS Spark 20 M microplate reader (Tecan, Männedorf, Switzerland). For the determination of the standard curve, a stock solution of 10% w/v of the following monosaccharides, based on the carbohydrate composition of SPI, was used: Rhamnose (55%), Ribose (12%), Xylose (6%), Mannose (4%), Galactose (7%), and Glucose (16%) (Chaiklahan et al., 2013). The protein content was determined with the DUMAS method (nitrogen-to-protein conversion factor for SPI: 6.21) (Safi et al., 2013) using an elemental (CHNS) analyser (Elementar Vario Cube, Langensenbold, Germany). Lipids were extracted with n-hexane and determined gravimetrically. The compositional profile of SPI is given in Table 1.

2.4. Preparation of the probiotic lyophilisates

For the preparation of the probiotic lyophilisates, the appropriate amount of protein powder (SPI, PPI or WPI) was dispersed into MilliQ water (10% wt.) under gentle stirring using an IKA GmbH stirrer (Staufen, Germany). The dispersions were stirred overnight to ensure the complete hydration of the proteins and were then homogenized twice at 800 bar. Afterwards, maltodextrin (12% wt.), trehalose (4% wt.), and glucose (1% wt.) were added as cryoprotectants, and the pH of the protein dispersions was adjusted to pH 7 with NaOH 0.1 M. The obtained solutions were heat-treated at 80 °C for 20 min in a shaking water bath (SW22, Julabo, Seelbach, Germany) and then cooled down to 4 °C prior to the inoculation with LGG cells.

Table 1
Proximate composition (g per 100 g dry matter) and extraction yield (%) of spirulina protein isolate (SPI).

Extraction Yield (%)	13.5 ± 1.9
Ash	6.3 ± 1.6
Total carbohydrates	8.1 ± 0.6
Protein	81.9 ± 3.1
Lipids	3.7 ± 3.5

The probiotic inocula were prepared according to Hellebois et al. (2023). Each protein solution was inoculated with the LGG cells to achieve a final microbial load of approx. 10 log CFU g^{-1}. Then, 1 mL aliquots of the LGG inoculated solutions were transferred into sterile 24-well microplates (CELLSTAR, Greiner Bio-One, Frickenhausen, Germany) and either deep-frozen at −80 °C for 2 h (−NT) or left to ferment at 37 °C until a pH 4.5 was reached ($t_{pH4.5}$ = 4 h, 1.5 h, 1.5 h for WPI, PPI, SPI, respectively) and then, cryogenically processed as mentioned above (−F). Ultimately, the samples were freeze-dried for 40 h (main stage: 0.120 mbar for 18 h; final stage: 0.010 mbar for 22 h).

2.5. Physicochemical and microstructural characterisation of the probiotic lyophilisates

2.5.1. Protein secondary structure

Fourier-Transform Infrared Spectroscopy (FTIR) analyses were performed using an Optics Vertex spectrometer (Bruker, Billerica, MA, United States) in the Attenuated Total Reflectance (ATR) mode with a diamond crystal. 50 scans were used for each spectrum. The baseline was measured without the sample and then subtracted from the sample spectra. The spectra were analysed within the wavenumber range of 4000 to 500 cm^{-1}. For the analysis of the secondary conformational stage of the protein, the amide I region (i.e., 1600 – 1700 cm^{-1}) was deconvoluted using Origin2019b (Jackson & Mantsch, 1995).

2.5.2. Water vapour sorption isotherms

The water vapour sorption isotherms of the probiotic lyophilisates were gravimetrically determined. Initially, the fresh probiotic lyophilisates were preconditioned at $a_w = 0$ in controlled atmosphere cabinets containing P_2O_5. Then the desiccated samples were stored in various RH-controlled hermetically sealed Nalgene acrylic desiccator cabinets (ThermoFisher Scientific, Waltham, MA, United States) for 3 weeks at 20 ± 1 °C. The following saturated salt solutions were employed: LiCl (a_w = 0.11), CH_3CO_2K (a_w = 0.23), $MgCl_2$ (a_w = 0.33), K_2CO3 (a_w = 0.43), $Mg(NO_3)_2$, (a_w = 0.54), NaCl (a_w = 0.75), NH_4Cl, (a_w = 0.79), KCl (a_w = 0.85) and KNO_3 (a_w = 0.94). The obtained water vapour uptake data were fitted with the Guggenheim-Anderson-De Boer (GAB, Eq. (1)) equation (van den Berg & Bruin, 1981) using Origin2019b:

$$X = \frac{X_m C k a_w}{(1-k a_w)(1-k a_w + C k a_w)} \quad (1)$$

where X denotes the water content at the equilibrium relative humidity (ERH), X_m the water content at the monolayer, a_w the water activity, C a constant defining the free enthalpy difference between pure liquid water molecules and the monolayer and k is a constant correcting the properties of the multilayer molecules. The total surface monolayer S_0 was calculated from Eq. (1) as follows (Eq. (2)):

$$S_0 = X_m \frac{1}{M_{H_2O}} N_A A_{H_2O} = 3.5 10^3 X_m \quad (2)$$

where M_{H_2O} denotes the molecular weight of water (18 g mol^{-1}), A is the surface of a single water molecule (1.06 × 10^{-19} m^2) and N_A is the Avogadro number (6 × 10^{23} molecules mol^{-1}).

2.5.3. Thermophysical properties

Thermogravimetric (TGA) and differential scanning calorimetric

(DSC) analyses were performed as described in Hellebois et al. (2023). The TGA was carried out with a TGA2 STAR^e system (Mettler Toledo, Zurich, Switzerland) and a heating rate of 5 °C min^{-1} from 30 to 800 °C. Moreover, the first derivative (DTG) of the thermographs was constructed with Origin2019b.

A DSC 3+ System (Mettler Toledo, Zurich, Switzerland) with the following heating-cooling protocol was implemented for the DSC analysis: 1) heating from −30 to 150 °C, 2) isothermal hold at 150 °C for 5 min, 3) cooling to −30 °C, 4) heating from −30 to 150 °C. The heating – cooling ramps were carried out at a rate of 10 °C min^{-1}.

2.5.4. Scanning electron microscopy (SEM)

The microstructure analysis of the probiotic lyophilisates was conducted using a field emission scanning electron microscope (SEM, SU-70, Hitachi, Tokyo, Japan). Prior to imaging, the crushed lyophilised samples were fixed on carbon tape, mounted on aluminium stubs, and coated with a 5 nm layer of platinum using an ACE 600 coating system (Leica Microsystems, Wetzlar, Germany). The analysis was performed at an acceleration of 5 kV, a working distance of 15 mm, and magnifications of × 1000 and × 5000.

2.6. In vitro gastrointestinal digestion testing

2.6.1. In vitro digestion protocol

The INFOGEST v2.0 static *in vitro* gastrointestinal digestion protocol was applied (Brodkorb et al., 2019). In this case, 250 mg of probiotic lyophilisate, stored at 4 °C and a_w 0.11, were mixed with 4.75 mL of MilliQ to achieve a food matrix of approximately 5 g. The food matrix was diluted 1:1 with oral fluids containing α-amylase (75 U L^{-1}), followed by an incubation in a shaking water bath (SW22, Julabo, Seelbach, Germany) at 37 ± 0.1 °C and 100 min^{-1} for 3 min. For the gastric phase, the samples were diluted 1:1 with prewarmed (37 °C) gastric fluids containing lipase (60 U mL^{-1}) and pepsin (2000 U mL^{-1}) and the pH was adjusted to pH 2.5 ± 0.1 with 60 μL HCl 6 M, followed by an incubation of 120 min at 37 ± 0.1 °C and 100 min^{-1}. After the gastric phase, the samples were diluted 1:1 with prewarmed (37 °C) intestinal fluids containing pancreatin (200 U mL^{-1}) and the pH was increased to pH 7 ± 0.1 with NaOH 5 M. The samples were incubated for 120 min at 37 ± 0.1 °C and 100 min^{-1}.

2.6.2. Investigation of the colloidal changes

The particle size distribution, de Brouckere diameter ($d_{4,3}$) and span of the oral, gastric and intestinal digesta were investigated by static light scattering using the Mastersizer 3000 (Malvern Instruments, Worcestershire, United Kingdom). An appropriate volume of digesta was added to the MV cell, aiming to reach 5 – 8% of laser obscuration, and filled with MilliQ. The background and sample measurement intervals with red and blue light were set at 10 s and 10 s, respectively. The measurement was repeated five times. The refractive indices for the dispersant, SPI, PPI and WPI were set at 1.33, 1.47, 1.52 and 1.45, respectively (Ahmed & Kumar, 2022; Moll et al., 2022).

To visualise the protein microstructure across all digestion stages a Confocal Laser Scanning Microscope (CLSM, LSM 880, Zeiss, Jena, Germany) equipped with a × 40 lens was used. Aliquots of 1 mL obtained at the end of each digestive step were mixed with 10 μL of Fast Green (λ_{Ex} = 633 nm, λ_{Em} = 635 – 680 nm) and 300 μL of the mixture was transferred into eight-chambered microscope slides (Nunc Lab-Tek II, Thermo Fisher Scientific, Waltham, MA, United States). The slides were then preserved on ice until the start of the analysis.

2.7. Microbiological assessment

2.7.1. Quantification of the total viable counts (TVC)

To quantify the TVC of LGG, 1 mL of probiotic solution or approximately 250 mg of lyophilisate were homogeneously mixed with 9 mL of PBS in a stomacher bag (MiniMix 100 W, Interscience, Roubaix, France), followed by serial log-dilutions. For the TVC after the gastric and intestinal phases, an appropriate amount of sample (minimum 3 mL) was mixed in a stomacher bag and ten-fold diluted. The samples were plated using the pour-plate method and incubated at 37 ± 1 °C for 48 h. A Scan 300 automatic colony counter (Interscience, Roubaix, France) was used to determine colony-forming units (CFU). All the counts were expressed on a dry basis.

2.7.2. Storage stability testing

For the investigation of the storage stability of the probiotic lyophilisates, the samples were stored under aerobic conditions at different temperatures and relative humidities in hermetically sealed boxes immediately after freeze-drying. Temperatures of 4, 20, and 37 ± 0.5 °C, along with a constant water activity of 0.11, were used to investigate the impact of temperature on LGG's viability. The influence of water activity on the viability was tested at a_w = 0.11 and 0.54, both at 20 ± 0.5 °C. Solutions of saturated salts (LiCl: a_w = 0.11 and $Mg(NO_3)_2$: a_w = 0.54) were used to create different relative humidities. The total viable counts (TVC) were determined as mentioned above.

In order to determine the cells' inactivation kinetics, the derived data was fitted with the Weibull model as described in Eq. (3)(van Boekel, 2009):

$$\log S(t) = -\frac{1}{2.303}\left(\frac{t}{\alpha}\right)^{\beta} \quad (3)$$

where S(t) is defined as the survival ratio S(t) = N(t) N_0^{-1}, t is the corresponding time (days), α is a scale parameter and β denotes the shape parameter.

2.7.3. LGG viability during in vitro digestion

The inactivation of cells during *in vitro* digestion was qualitatively examined using CLSM. Aliquots of 1 mL, obtained at the end of the oral, gastric, and intestinal phases, were combined with 1.5 μL of propidium iodide (20 mM, λ_{Ex} = 488 nm, λ_{Em} = 585 – 640 nm) to stain inactivated cells and 1.5 μL of SYTO9 (3 mM, λ_{Ex} = 488 nm, λ_{Em} = 498 – 550 nm) used for staining viable cells (LIVE/DEAD BacLight, Thermo Fisher Scientific, Waltham, MA, United States). The stained samples were subsequently analysed as outlined in section 2.6.2.

To evaluate the LGG TVC in a quantitative manner within gastric (t = 120 min) and intestinal fluids (t = 120 min), a sufficient volume of the samples (min. 3 mL) was mechanically homogenized in a stomacher bag (Minimix 100, Interscience, Roubaix, France), followed by serial dilutions. The pour-plate method was employed thereafter to enumerate viable LGG cells, as detailed in section 2.7.1.

2.7.4. Cell adhesion properties

2.7.4.1. Preparation of the intestinal epithelium co-culture model. The human colon cancer Caco-2 cell line sub-clone TC7 (Caco-2/TC7) and HT29-MTX cells lines were used to prepare a co-culture model. The cells were seeded on 6-well microplates and eight-chambered microscope slides (Nunc Lab-Tek II, Thermo Fisher Scientific, Waltham, MA, United States). Dulbecco's Modified Eagle Medium-Glutamax (DMEM-Glutamax, Invitrogen) supplemented with 10% fetal bovine serum (Invitrogen, Merelbeke, Belgium) was used as growing medium and refreshed every two days. The co-culture model was incubated at 37 ± 0.5 °C in a humidified incubator with 10% CO_2 in the atmosphere. After 14 days the cells were matured and washed twice with 2 mL of PBS prior to fixating the cells with 2.5% vv. of glutaraldehyde in PBS for 30 min, to prevent the cells of being digested when intestinal enzymes are present. Finally, the fixed cells were washed twice with 2 mL of PBS and stored with PBS at 5 °C until further use.

2.7.4.2. Investigation of adhered LGG cells. To examine the adhesion behaviour of LGG cells on the intestinal epithelium, the wells of the

microplates and eight-chambered microscope slides were removed from PBS and filled with 2.5 mL and 300 μL of intestinal digesta, respectively. The samples were incubated for 120 min at 37 ± 1 °C in an orbital shaker (100 rpm) (Świątecka et al., 2010) and washed twice with PBS afterwards. The adhered bacteria were microscopically investigated by means of CLSM and a × 40 objective. The viable and dead LGG cells were stained with SYTO9 and propidium iodide, respectively. To estimate the TVC of the adhered cells, the epithelium was diluted with 2.5 mL PBS, scraped off from the microplate and mechanically broken. Afterwards, the bacteria suspension was plated on MRS agar plates as described in section 2.7.1.

2.8. Statistical analysis

Origin2019b (OriginLab, Northampton, MA, United States) was used to conduct each statistical analysis. The significant differences were determined by two-way ANOVA ($p < 0.05$) and Tukey's post-hoc means comparison test was used for the differentiation of the values.

3. Results and discussion

3.1. Secondary structure of the protein isolates and probiotic lyophilisates

To assess the impact of the protein type and pre-fermentation step on the chemical structure of the probiotic xero-formulations, the free LGG cells, protein isolates and the LGG conveying xero-carriers were analysed by FTIR (Fig. 2). According to Fig. 2A, all systems exhibited a similar FTIR spectral pattern, with the peaks associated with the secondary structure conformation of the proteins, i.e., amide I, 1700 – 1600 cm^{-1} (C═O stretching vibrations of peptide bonds), amide II, 1500 – 1600 cm^{-1} (N–H bending/C–N stretching modes) and amide III, 1200 – 1400 cm^{-1}, (N–H in-plane and C–N stretching vibrations) regions, to be among the most abundant ones. Interestingly, the characteristic peak at 1238 cm^{-1} identified in the FTIR spectra of the lyophilised LGG cells was not observed in any of the probiotic formulations' spectra, indicating a satisfactory encapsulation of the LGG cells in the wall material. Indeed, Hlaing et al. (2017) reported a peak at 1210 – 1240 cm^{-1} in freeze- and spray-dried LGG cells, which was assigned to the asymmetric stretching bands of the phosphodiester groups of nucleic acids. In addition, the peaks identified at 1147, 1101, 1076, 1018 and 993 cm^{-1} are characteristic of the carbohydrate matter, i.e., maltodextrin (Kim et al., 2023), trehalose and glucose (Hellebois et al., 2023).

The deconvolution of the amide I peak allowed the identification of three major secondary structure conformations assigned to β-sheet (1630 – 1623 cm^{-1}), α-helix (1655 – 1651 cm^{-1}) and aggregated β-sheet (1691 – 1980 cm^{-1}). According to Fig. 2B, SPI exerted a predominant β-sheet structure conformation (i.e., 67% β-sheet, 18% aggregated β-sheet, 14% α-helix), whilst WPI (56% β-sheet, 5% aggregated β-sheet, 39% α-helix) and PPI (49% β-sheet, 11% aggregated β-sheet, 40% α-helix) exhibited a more even proportion between the inter- and intramolecular stabilised polypeptide chains.

As for the probiotic lyophilisates, a significant ($p < 0.001$) increase in the proportion of the β-sheet at the expense of α-helix conformation was observed. Furthermore, implementing the pre-fermentation step further increased the prevalence of the β-sheets. Both the freezing and dehydration steps during lyophilisation can induce the modification of the proteins' secondary structure (Roy & Gupta, 2004). Although deploying cryoprotective and lyoprotective sugars such as sucrose, trehalose and lactose may protect the secondary structure of proteins via a H-bonding stabilising mechanism (Roy & Gupta, 2004), it was not possible to detect any stabilisation effect in the presence of trehalose and/or glucose even when native protein lyophilisates were tested (data not shown). Therefore, it is assumed that globular proteins such as phycocyanin (Spirulina), β-lactoglobulin (whey), vicilin and legumin (pea), undergoing denaturation during the heat treatment and fermentation steps, exhibit an impaired ability to maintain their structure conformational state (in solution) during the lyophilisation process.

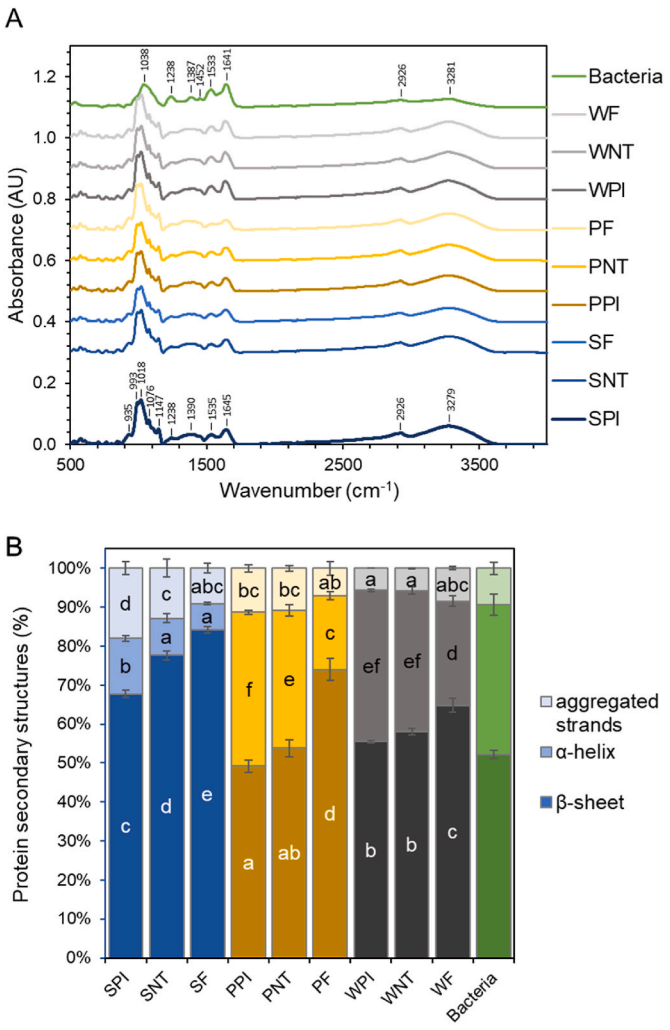

Fig. 2. Influence of protein composition (S = spirulina, P = pea, W = whey) and precursor treatment (NT = non-treated, F = fermented) on the FTIR spectra of lyophilisates containing LGG cells (A) and prevalence of the protein secondary structures (B). [a-f]Different letters denote a significant difference according to Tukey's post hoc means comparison test ($p < 0.05$).

3.2. Microstructural aspects of the probiotic lyophilisates

As expected, the type of the protein isolate was influential on the microstructural conformation of the lyophilisates (Fig. 3). All SPI probiotic lyophilisates exhibited a rough surface consisting of irregularly interconnected protein aggregates resembling the microstructure of fermented milk. On the other hand, the PPI lyophilisates exhibited a less aggregated and more compact microstructure with small globular conformations protruding. Contrary to the SPI and PPI lyophilisates, the morphological characteristics of the WPI exemplars were clearly influenced by the pre-fermentation step. As illustrated in Fig. 3 A5, B5 the lyophilisates prepared by the non-fermented biopolymer dispersions exhibited a smooth, non-porous, crystalline-like microstructure with sharp edges, which is very similar to the observations of Betz et al. (2012). In contrast, the WF lyophilisates exhibited a highly macroporous, honeycomb-like lacunar microstructure composed of rough surface interconnected vessels (Fig. 3 A6, B6). As we have recently shown (Hellebois et al., 2023), the pre-gelation of WPI based aqueous solutions (at $c \sim c_{LGC}$ i.e., 12% wt.) regulates sterically the growth of ice crystals (at $T > T_{vitrification}$), resulting in the formation of spongy

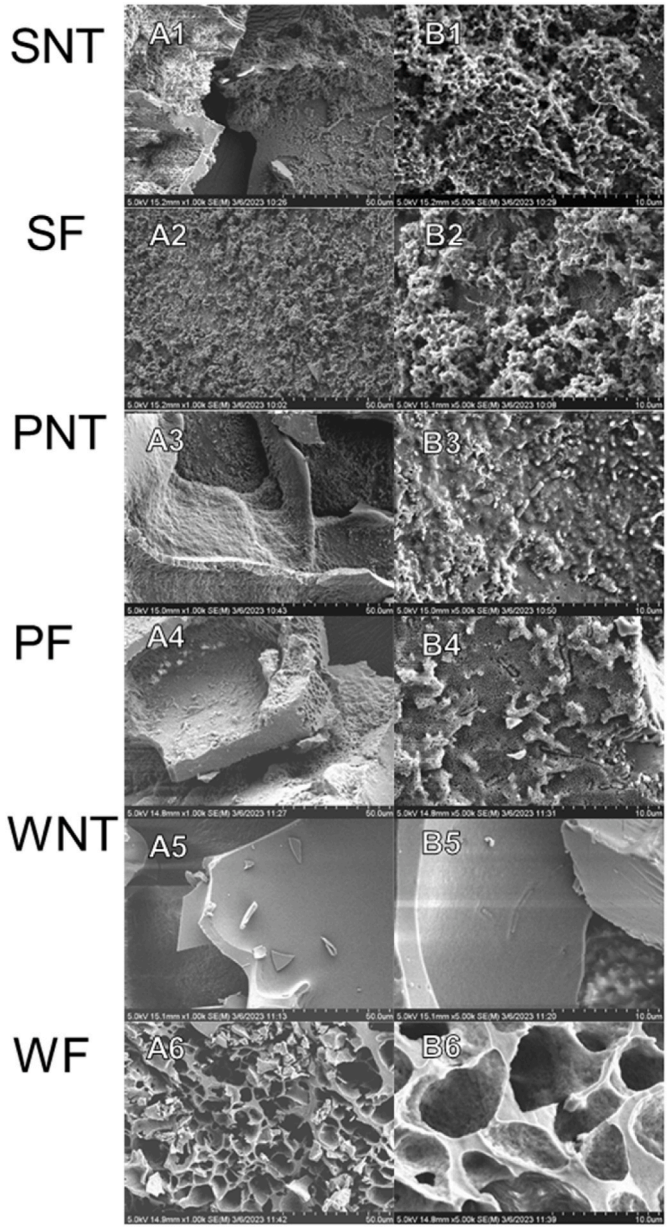

Fig. 3. SEM micrographs of the lyophilisates encapsulating LGG wt cells microstructure as influenced by protein composition (S = spirulina, P = pea, W = whey) and precursor treatment (NT = non-treated, F = fermented) at a magnification of × 1000 (A) and × 5000 (B).

macroporous cryogels. Although in the present work $c_{WPI} < c_{LGC}$, the presence of cosolvents (i.e., sugars and maltodextrin) promoted the development of rigid elastic gels most probably due the supramolecular stabilisation of the network via hydrophobic or hydrogen bonding interactions (Nicolai, 2019). Despite their ability to form acid gels, SPI and PPI resulted in rather weak gels (G' ~ 80–100 Pa for SPI and PPI compared to G' ~ 900 Pa, in the case of the WPI) in the form of free-flowing acid aggregated fractals, which were not able to constrain the growth of the porogens leading to rugged flaky features. This is due their differences regarding the isoelectric point (pI) i.e., pH ~ 4.5, pH 3.5 – 5.0 and pH 3–5 for WPI, PPI and SPI, respectively (Benelhadj et al., 2016; Chen et al., 2019; Hansen et al., 2022; Pelegrine & Gasparetto, 2005).

Regarding the LGG cells engrafting efficacy, no bacterial cells were detected on the surface of the SPI and fermented WPI lyophilisates, implying satisfactory matrix – LGG cell adhesion properties. However, SEM micrographs of the lyophilisates with PPI revealed the presence of a limited number of LGG cell chains on the lyophilisates surface, which could make them more vulnerable to sublethal cell injuries (Fig. 3 B3-5). Yet, the LGG cell – matrix adhesion properties will be discussed in a future work.

3.3. Water vapour sorption properties and thermal stability

The residual moisture content of the probiotic lyophilisates ranged from 2.1 to 2.9 g per 100 g, which falls within the technical requirements of anhydrobiotic formulations (< 2 – 3% wt.) as reported by Aschenbrenner et al. (2015).

For the determination of the water vapour sorption isotherms all probiotic powders were dehumidified for 2 weeks in an inert gas (argon) glove box under absolute dryness (a_w = 0.003, 1 bar) followed by humidification at different ERH conditions. As shown in Fig. 4, the probiotic powders exhibited a sorption isotherm type II according to the BET classification, indicating a non-porous nature. The equilibrium water content X_e was increased steadily in the low to intermediate a_w region, whereas an inflection point at a >0.7 was detected due to the enhanced hygroscopicity resulting from the presence of hygroscopic amorphous plasticizing sugars, leading to capillary saturation (Hartmann & Palzer, 2011). By fitting the GAB model (eq. (1)) to the moisture – a_w data, the monolayer water content (X_m) and surface (S_0) values were calculated (eq. (2), Table 2). No significant differences in the X_m and S_0 values between the non-treated (X_m = 5.09 g 100 g^{-1}, S_0 = 178.3 m^2 g^{-1}) and fermented (X_m = 5.22 g 100 g^{-1}, S_0 = 182.9 m^2 g^{-1}) lyophilisates were found. On the other hand, the PPI-based lyophilisates demonstrated the highest ($p < 0.05$) monolayer water content (X_m = 5.34 g 100 g^{-1}) when compared to the SPI and WPI exemplars (X_m = 5.11 and 5.03 g 100 g^{-1}, respectively). The X_m value represents the amount of water chemisorbed through hydrogen bond bridging to the polar and ionic groups of the wall materials (van den Berg & Bruin, 1981). Various factors, such as the chemical composition, supramolecular structure, and microstructural aspects of the powders, play a crucial role in influencing the water sorption dynamics (Hartmann & Palzer, 2011). In the context of anhydrobiotic formulations, X_m holds significant importance alongside the critical water activity in determining the

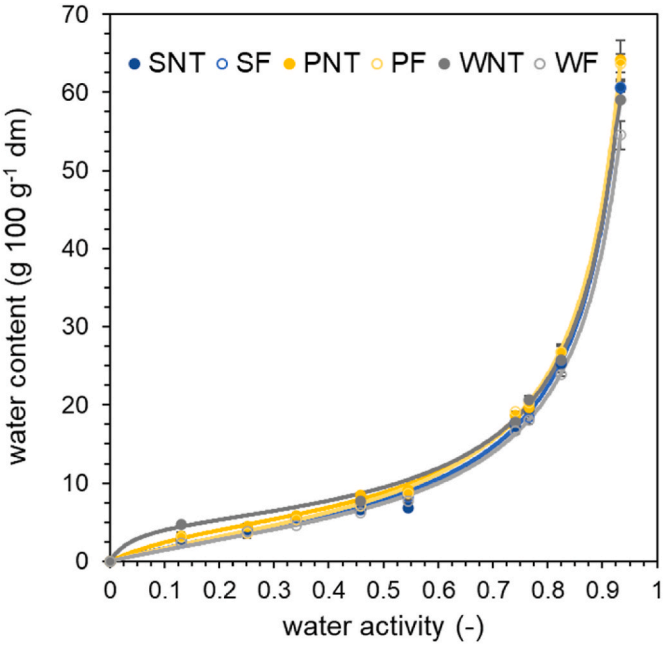

Fig. 4. Influence of protein composition (S = spirulina, P = pea, W = whey) and precursor treatment (NT = non-treated, F = fermented) on the water vapour adsorption isotherms of lyophilisates containing LGG cells.

Table 2
Influence of lyophilisate protein composition (S = spirulina, P = pea, W = whey) and precursor pre-treatment (NT = non-treated, F = fermented) on the kinetic parameters of the GAB model.

	X_m (g 100 g^{-1})	C (−)	k (−)	S_0 (m^2 g^{-1})	R^2 (−)
SNT	5.1 ± 0.2^{ab}	3.5 ± 0.5^{a}	0.98 ± 0.004^{ab}	179.2 ± 8.2^{ab}	0.997
SF	5.1 ± 0.1^{ab}	3.9 ± 0.4^{a}	0.98 ± 0.000^{ab}	178.3 ± 1.7^{ab}	0.999
PNT	5.1 ± 0.0^{ab}	6.7 ± 1.2^{b}	0.99 ± 0.004^{b}	180.2 ± 1.4^{ab}	0.999
PF	5.5 ± 0.1^{b}	3.4 ± 0.1^{a}	0.98 ± 0.001^{ab}	193.7 ± 2.0^{b}	0.999
WNT	5.0 ± 0.1^{a}	23.2 ± 0.1^{c}	0.98 ± 0.001^{ab}	175.5 ± 2.3^{a}	0.998
WF	5.0 ± 0.1^{a}	3.2 ± 0.2^{a}	0.98 ± 0.002^{a}	176.5 ± 3.3^{a}	0.998

X_m: monolayer water content; C: constant describing the difference between the free enthalpy of the monolayer and liquid water molecules, k: constant correcting the properties of the multilayer molecules, S_0: total surface monolayer. $^{a-c}$Different letters denote a significant difference according to Tukey's post hoc means comparison test ($p < 0.05$).

biological activity of living probiotic cells (Passot et al., 2012). The X_m values calculated in this study align with those reported for protein-maltodextrin lyophilisates (Hoobin et al., 2013; Ying et al., 2012).

Furthermore, the thermal stability of the dehumidified probiotic lyophilisates was assessed using TGA, revealing four major thermal events (Fig. 5, Table 3). These events corresponded to water evaporation (74 − 82 °C, 2.2 < Δm < 2.9%), and decomposition of low molecular oligosaccharides (219 − 237 °C, 8.1 < Δm < 13.4%), protein/maltodextrin (277 − 288 °C, 43.6 < Δm < 66.7%), and maltodextrin/mineral matter (435 − 469 °C, 9.8 < Δm < 25.8%). These findings align with previous studies (Hellebois et al., 2023; Paula et al., 2022; Saavedra-Leos et al., 2015). Besides, a pyrolytic decomposition event of the residual matter was observed at 53 − 622 °C (5.7 < Δm < 29.8%). Interestingly, in the case of SPI lyophilisates, an additional thermal event at 176 °C was recorded. This event was attributed to the devolatilization of heat-labile pigmentation bioactives, such as chlorophylls and carotenoids (Kang et al., 2019; Pinho et al., 2022).

3.4. Colloidal changes during simulated in vitro digestion conditions

The probiotic lyophilisates underwent *in vitro* digestion adopting the static INFOGEST v.2 model, and the colloidal changes taking place in each phase (oral, gastric, and intestine) were monitored using CLSM (Fig. 6) and SLS (Fig. 7). The volume weighted particles mean size ($d_{4,3}$) as well as the span are summarised in Table 4. As illustrated in Fig. 6A, admixing the probiotic lyophilisates with the artificial saliva resulted in their quick disintegration into partially hydrated microparticles having a $d_{4,3}$ ranging from 6.6 to 214.0 μm. The protein isolate type and the implementation of the acidification step were influential on the heterogeneity of the particles present in the simulated oral boluses. All SPI-based oral boluses exhibited the highest uniformity (monomodal particle size distribution, $d_{4,3}$ = ~23 μm), whilst the WNT and PNT exemplars comprised diverse particle populations. The implementation of the pre-fermentation step significantly hampered ($p < 0.001$) the ability of the WF and PF probiotic lyophilisates to undergo extensive disintegration on their exposure to artificial saliva, resulting in a uniform suspension of insoluble large protein aggregates ($d_{4,3}$ = 214.0 and 51.6 μm for WF and PF, respectively). With the exception of the WNT systems, the release of free LGG cells into the bulk aqueous phase was found to be highly restricted. This restriction appears to be directly associated with the low volume density of the oral boluses in advanced disintegrated particles with a size of $d_{4,3}$ less than 1−3 μm.

A distinct colloidal response to low pH and pepsin was observed

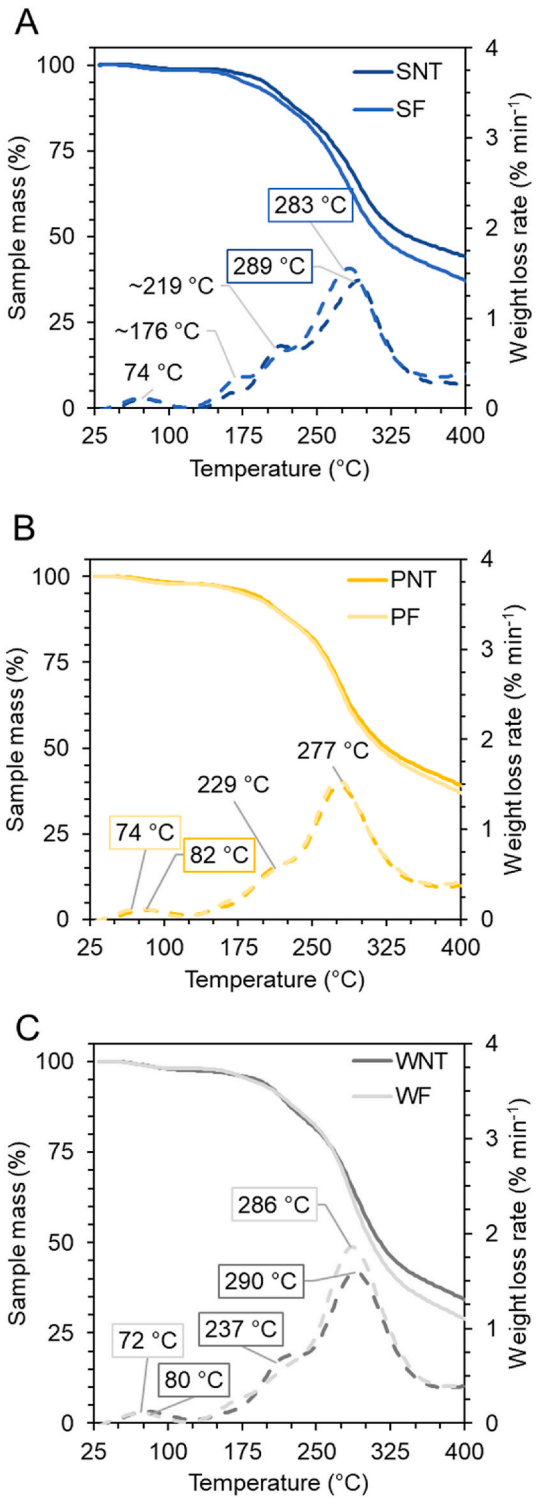

Fig. 5. Thermal properties assessed by TGA (continuous lines) and DTG (dashed lines) of lyophilisates containing LGG cells as influenced by their protein composition (S = spirulina, P = pea, W = whey) and precursor treatment (NT = non-treated, F = fermented).

upon admixing the oral boluses with simulated gastric fluids (Fig. 6B). The SPI-based formulations retained their colloidal uniformity, with monomodal particle size distributions, experiencing only a slight increase in their mean size (27.0 and 23.4 μm for SNT and SF, respectively). Similarly, the PPI-based formulations demonstrated good colloidal uniformity. However, the mean size of the protein particles

Table 3
Influence of lyophilisate protein composition (S = spirulina, P = pea, W = whey) and precursor pre-treatment (NT = non-treated, F = fermented) on the mass loss (%) occurring during the different detected thermal events.

T (°C)	SNT	SF
	mass loss (%)	mass loss (%)
74 ± 4	2.2 ± 0.1	2.1 ± 0.1
176 ± 1	2.4 ± 0.4	4.3 ± 0.2
219 ± 7	11.2 ± 0.1	8.1 ± 0.6
287 ± 4	43.6 ± 0.0	46.8 ± 0.5
435 ± 14	9.8 ± 0.5	15.4 ± 2.8
530 ± 3	29.8 ± 0.3	23.3 ± 2.6
T (°C)	PNT	PF
	mass loss (%)	mass loss (%)
79 ± 4	2.5 ± 0.0	2.6 ± 0.0
229 ± 1	11.0 ± 0.5	11.6 ± 0.5
277 ± 1	44.7 ± 0.5	45.7 ± 0.8
453 ± 6	16.2 ± 1.4	19.7 ± 2.3
547 ± 2	25.5 ± 1.3	20.1 ± 3.7
T (°C)	WNT	WF
	mass loss (%)	mass loss (%)
76 ± 4	2.9 ± 0.02	2.3 ± 0.2
237	13.4 ± 0.1	Nd
288 ± 2	46.5 ± 0.4	66.7 ± 0.7
469 ± 2	25.8 ± 1.8	25.2 ± 0.0
622 ± 5	11.4 ± 2.3	5.7 ± 0.9

nd: not detected.

increased (63.7 and 75.7 μm for PNT and PF, respectively), indicating their greater responsiveness to gastric fluids. In the case of the WF-based gastric chymes, there was a significant decrease in the aggregates' mean size from 214 to 6 μm, resulting from the reduction in the volume density of the particle population above 100 μm. The colloidal transformation of the protein-rich aqueous systems during gastric processing is primarily associated with the occurrence of pepsin and acid-mediated aggregation, as well as pepsin-induced cleavage of the proteins (Loveday, 2022). Although pepsin clotting has been exclusively reported in the case of micellar casein (Ye, 2021), its occurrence in whey, pea and microalgal protein systems is considered unlike. On the other hand, the acid-gelation of proteins is closely linked to their isoelectric points (Augustin & Hemar, 2009). With the exception of SPI, which exhibits a very low pI (~2.8 – 3.5) explaining its low colloidal responsiveness to the highly acidic environment of the gastric fluids, WPI and PPI are characterised by significantly higher pIs (i.e, ~3.5 – 5.0 and 5.2 for PPI and WPI, respectively) promoting to some extent the acid coagulation of the proteins in the -NT based boluses as well as the microstructural rearrangement of the acid aggregate fractals already present in the –F bolus exemplars.

The exposure of SPI and PPI gastric chymes to simulating jejunum fluids was accompanied by a significant reduction in the mean particle size (Fig. 6C, $d_{4,3}$ = 13.7 – 38.2 μm). In contrast, SLS analysis of WPI-based chymes did not reveal any remarkable colloidal changes ($d_{4,3}$ 6.6 – 15 μm). Based on the volume density pattern of the bi- or trimodal particle size distributions of the digesta, the population of the intermediate-sized particles ($1 < d_{4,3} < 100$ μm) was the most affected by the pancreases, which also explains the significant enrichment of free LGG cells in the bulk aqueous phase. Similar behaviour has been observed in other protein-based cryostructurates (Hellebois et al., 2024).

3.5. Microbiological measurements

3.5.1. Lyostabilising effects of the protein isolates on LGG cells

The impact of the freeze-drying process on the total viable counts (TVC) of LGG is depicted in Fig. 8. Generally, the LGG TVC losses ranged from 0.07 to 0.70 log CFU g^{-1}, with the highest ($p < 0.001$) LGG cellular lethality to be encountered in the fermented lyophilisates (i.e., −0.33 to −0.70 log CFU g^{-1}) compared to the non-treated exemplars (i.e., −0.07 to −0.13 log CFU g^{-1}). Wang et al. (2005) reported that the cryotolerance of *Lactobacillus acidophilus* (at −20 °C) was decreased at higher fermentation temperatures (42 °C) and low pH endpoint (i.e., 4.5). Recently Cui et al. (2018) demonstrated that the decrease in the cryotolerance of Lactobacilli during freeze-drying is associated with changes in membrane fatty acid composition (i.e., increased ratio of unsaturated to saturated fatty acids) due to adaptation to the acidic conditions, as well as with changes in the physical state of the membrane lipids, i.e., damaged cell membranes or reduced membrane fluidity. Nonetheless, the severity of the impact of fermentation on the cryotolerance of probiotics is prevalently strain dependent (Capozzi et al., 2011).

As concerns the impact of the protein isolates, the PPI demonstrated the best lyostabilising performance ($p < 0.01$; −0.22 log CFU g^{-1}) compared to SPI (−0.35 log CFU g^{-1}) and WPI (−0.41 log CFU g^{-1}). Our findings confirmed the satisfactory lyostabilising efficacy of the wall materials, since TVC losses up to one log CFU g^{-1} are commonly reported for anhydrobiotics produced via freeze-drying (Pehkonen et al., 2008; Wang et al., 2004; Ying et al., 2010). The lyostabilising capacity of proteins is primarily associated with their ability to preserve the fluid crystalline state of the cell's membrane during the desiccation process by binding water via hydrogen bonding, close to the hydrophilic interface of the polar heads of the phospholipid bilayer. Interestingly, a good correlation ($r = 0.99$, $p < 0.001$) between the water affinity (wettability) of the protein isolate powders and LGG cell inactivation was found (Suppl. Fig. 1). This suggests that the excellent lyostabilising performance of the pea isolate may arise from its superior ability to retain water close to the bacterial cell interface, preserving the cells' membrane fluidity during the desiccation step. This was confirmed by determining the contact angle between the protein isolates and water (120.3°, 66.9°, and 108.5° for SPI, PPI, and WPI, respectively). In addition, macromolecular lyoprotectants such as polysaccharides and proteins may induce the elevation of the glass transition (T_g) point of the freeze-concentrated precursors allowing their vitrification at higher temperatures and thus, minimising the cellular injuries due to uncontrolled ice crystal ripening. According to the DSC measurements (data not shown), the protein type did not significantly affect the T_g of the freeze-concentrated systems nor modified the ice crystals uniformity (T_g ~ −31 °C).

3.5.2. Viability of LGG cells under controlled storage conditions

To gain insight into their shelf-life aspects, the probiotic lyophilisates were stored under controlled ERH (aw = 0.11 and 0.54) and temperature (T = 4, 20, and 37 °C) conditions. Due to the non-linear time-dependent inactivation of the LGG cells during the accelerated storage trials, we fitted the Weibull model (Eq. (3)) to the TVC-storage time data and calculated the parameters α (characteristic time – in days) and β (dimensionless) (Fig. 9, Table 5). Nonetheless, it was not possible to fit either the Weibull model or the first-order kinetic model with the obtained data at a storage temperature of 4 °C, which was attributed to the exceptionally high survivability of the LGG under chilling conditions. As demonstrated in van Boekel (2002), the β parameter is either indicative of the cells' adaptation to the applied stressor ($\beta < 1$) or the accumulated cellular damage ($\beta > 1$). On the other hand, the α parameter denotes the time required for a log (1/e) decline in the living cell's load to be achieved. According to the ANOVA findings, the increase in the storage temperature was accompanied by a significant ($p < 0.001$) increase in the β parameter values (β_T = 1.43 and 2.20 at 20 and 37 °C, respectively).

Nonetheless, it was not possible to calculate the activation energy (E_a) due to the poor modelling of the inactivation kinetics at the tested chilling conditions (4 °C). It is well established that the reciprocal to storage temperature survivability of probiotics is due to the acceleration

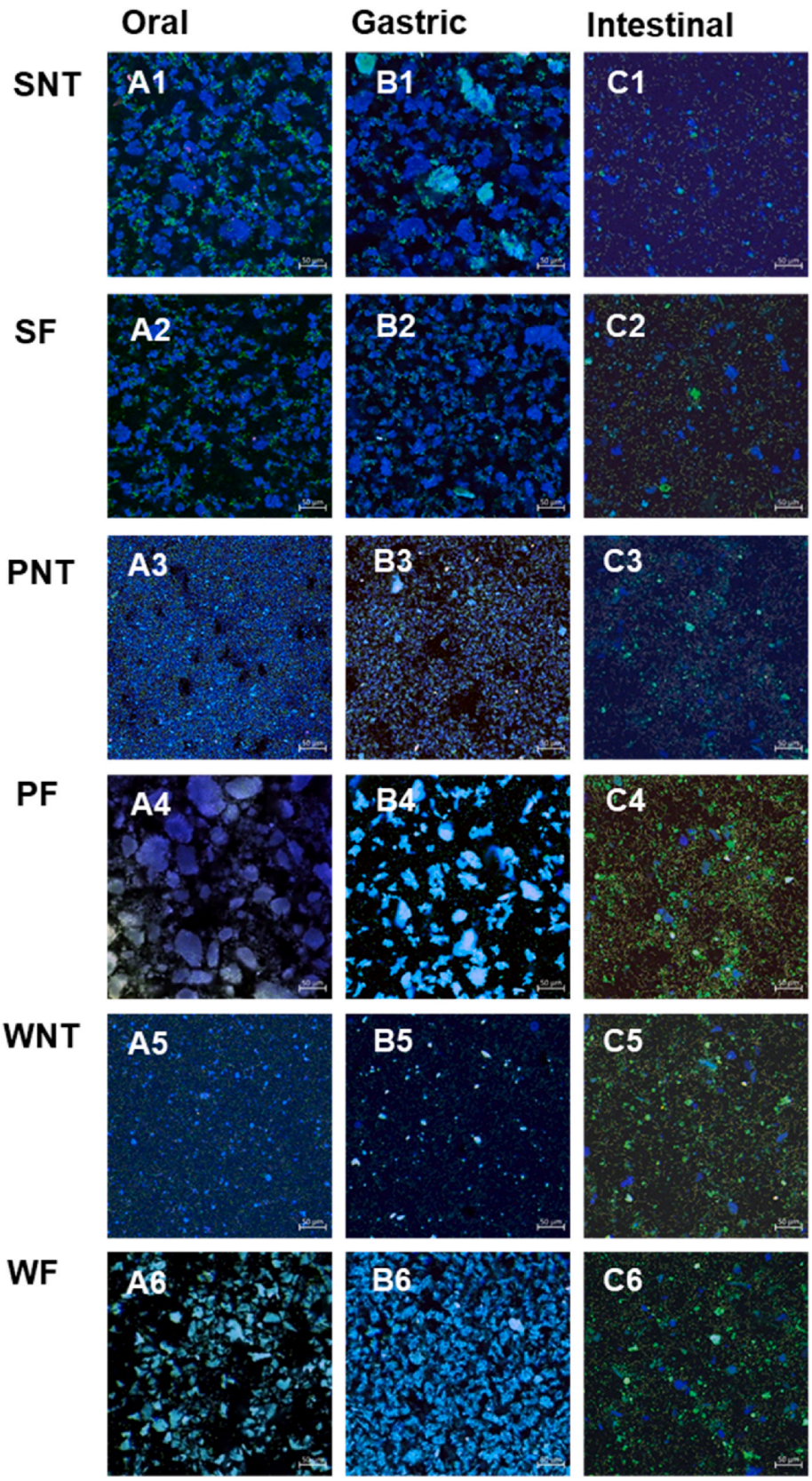

Fig. 6. Influence of protein composition (S = spirulina, P = pea, W = whey) and precursor treatment (NT = non-treated, F = fermented) on microstructural features of the boluses (A, t = 3 min), gastric (B) and intestinal (C) chymes (t = 120 min, each) on lyophilisates containing LGG cells visualised by CLSM (× 20, green = life bacteria, red = dead bacteria, blue = protein).

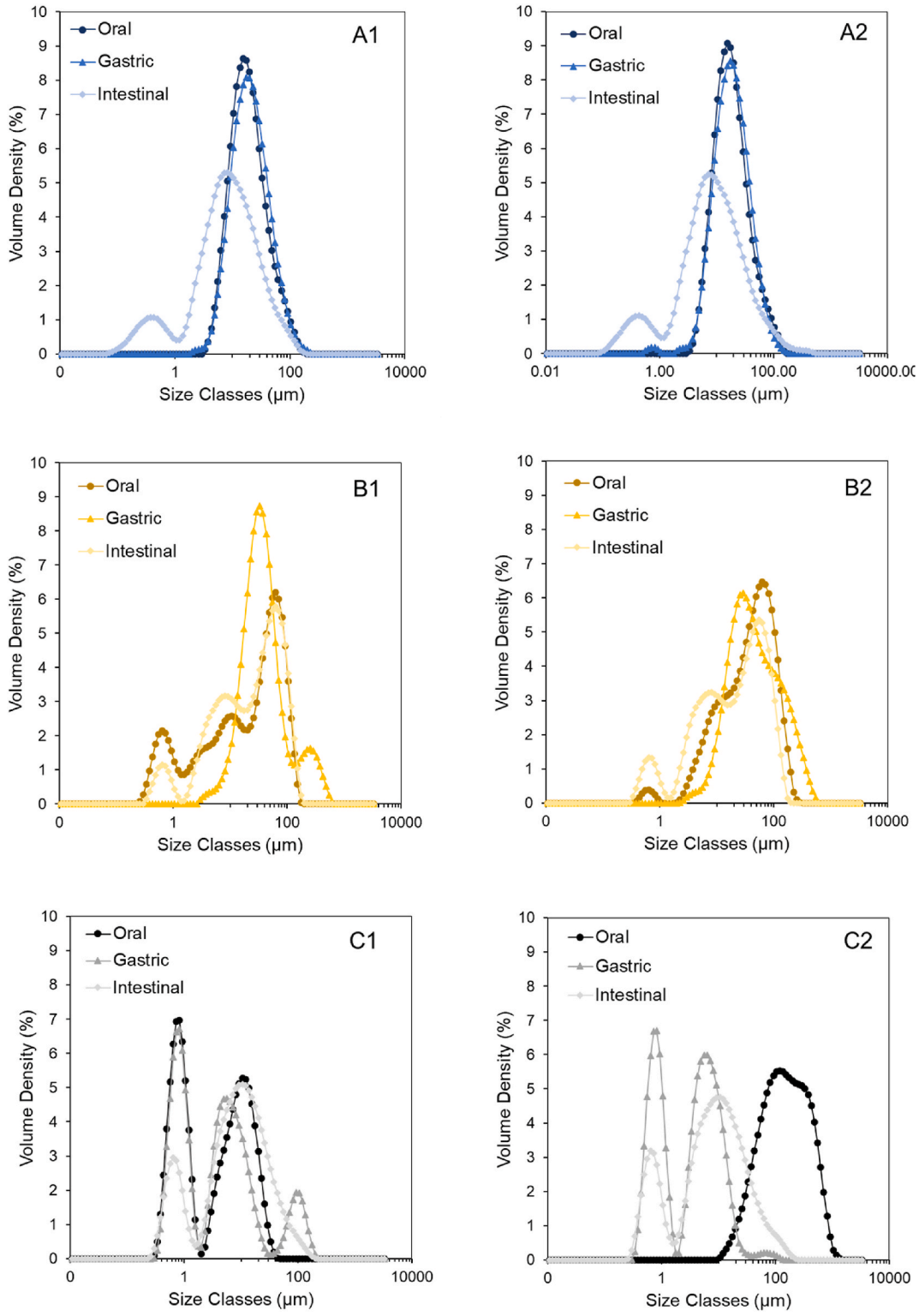

Fig. 7. Influence of protein composition (spirulina (A), pea (B) and whey (C) protein isolate) and precursor treatment (non-treated (1) and fermented (2)) on the particle size distribution of the boluses (t = 3 min), gastric and intestinal chymes (t = 120 min, each) on lyophilisates containing LGG cells.

of their metabolic activity. The elevation of the storage RH at 20 °C was associated with a substantial reduction in the kinetic parameters (β_{RH} = 2.20 vs. 0.94, α_{RH} = 92.9 vs. 3.51 days, for 11% and 54% ERH, respectively), both indicating the increased cellular lethality in systems stored at 54% RH. The pre-fermentation step was also significantly ($p < 0.001$) influential on the kinetic parameters, i.e., β = 2.43 vs. 1.23, α = 79.4 vs. 24.4 days, for NT and F, respectively. As for the impact of the protein isolate type, PPI offered the highest storage stability of the LGG cells compared to the SPI and WPI exemplars (i.e., β = 1.3 vs. 1.7 vs. 1.6, α = 22.4 vs. 48 vs. 37 days, for SPI, PPI, and WPI, respectively).

The inactivation dynamics of probiotics are primarily dependent on the genus, species, and strain (Capozzi et al., 2011). For instance, Meireles Mafaldo et al. (2022) reported that the TVC losses of *Lacticaseibacillus casei* and *Lacticaseibacillus acidophilus* encapsulated via freeze

Table 4
Influence of lyophilisate protein composition (S = spirulina, P = pea, W = whey) and precursor pre-treatment (NT = non-treated, F = fermented) on the volume weighted mean diameter $d_{4,3}$ (μm) and span (dimensionless) of the particles present in the oro-gastrointestinal chymes.

	$d_{4,3}$			Span		
	Oral	G120	I120	Oral	G120	I120
SNT	24.7 ± 0.7^{b}	27.0 ± 0.5^{c}	14.9 ± 0.4^{a}	2.4 ± 0.1^{A}	2.3 ± 0.0^{A}	4.3 ± 0.8^{A}
SF	23.4 ± 0.0^{b}	23.4 ± 1.0^{bc}	17.6 ± 4.3^{bc}	2.3 ± 0.0^{A}	2.1 ± 0.1^{A}	4.8 ± 1.4^{A}
PNT	35.9 ± 5.1^{c}	63.7 ± 12.0^{d}	38.2 ± 0.1^{c}	3.8 ± 1.3^{B}	3.8 ± 1.5^{A}	3.4 ± 0.0^{A}
PF	51.6 ± 4.7^{d}	75.7 ± 1.2^{e}	34.1 ± 2.0^{b}	2.7 ± 0.4^{A}	4.3 ± 0.3^{A}	3.8 ± 0.7^{A}
WNT	6.6 ± 0.2^{a}	15.3 ± 3.4^{b}	15.0 ± 0.3^{a}	3.9 ± 0.1^{B}	15.4 ± 8.1^{B}	4.3 ± 0.8^{A}
WF	214 ± 12.1^{e}	5.8 ± 1.3^{a}	16.0 ± 0.6^{a}	3.1 ± 0.2^{AB}	3.1 ± 0.8^{A}	4.8 ± 0.8^{A}

Different letters among rows denote a significant difference ($p < 0.05$) according to Duncan's multiple range test. $^{a\text{-}j}$small letters denote a significant difference within the samples for the de Brouckere mean particle size diameter. ^{A,B}capital letters denote a significant difference for the span.

drying in *Spirulina platensis* biomass amounted to 1.5 and 2.5 log CFU g^{-1} after 120 days of storage at 4 °C, which are generally substantially higher than those reported in the present work. In addition to the microbial factors, extrinsic parameters such as the storage ambient temperature, water activity, and oxygen content, as well as the composition, microstructural conformation, and physical state of the cell-conveying colloidal template, can also result in drastic changes in the inactivation kinetics of probiotics during storage (Flach et al., 2018; Mendonça et al., 2022). As mentioned above, all xero-templates allowed a satisfactory engrafting of the living LGG cells into their wall material, with a limited number of cells located on the outer part of the particulates (Fig. 3). With the exception of the WF lyophilisates, which could allow sufficient diffusion of oxygen and water vapour through their highly macroporous structure (Fig. 3 A6, B6), it was not possible to identify a clear interrelationship between the microstructural features of the lyophilisates and the achieved LGG preservation performance.

The impact of the composition of the wall material on the survivability of Lactobacilli can be related to potentially adverse effects due to the presence of inhibitory compounds e.g. chitosan, Ca^{2+} etc. (Yonekura et al., 2014; Yuan et al., 2022); yet this is unlikely as no inhibitory effects of the protein isolates on the LGG growth were detected. Moreover, the adhesion properties of the wall materials are known to control the spatial distribution and self-aggregation of the living cells in the conveying polymeric matrix, and therefore to modulate the ability of the cells to counteract the physicochemical stressors encountered during storage. For example, Guerin et al. (2018) demonstrated the preferential adhesion properties of LGG to β-lactoglobulin compared to other whey proteins (e.g., α-lactalbumin, BSA) and micellar caseins via their surface biomolecules such as SpaCBA pili, EPS and other protein molecules. In view of this, the differences in the adhesion affinity of tested protein isolates to LGG cells could plausibly explain their superior survivability in the PPI-based substrates, though this needs further investigation.

The changes in the physical state (i.e., glassy to rubbery state transition) of the LGG cell conveying xero-template during storage due to water vapour adsorption, temperature fluctuation, wall material aging, etc., are probably among the most important extrinsic parameters that could eventually lead to cell lethality (Hellebois et al., 2024; Kurtmann et al., 2009; Ying et al., 2012). To gain insight into the impact of the hereby tested conditions, probiotic lyophilisates were conditioned at different relative humidities (11 and 54%) and aged for 1 month at an ambient temperature. Subsequently, the samples were analysed by means of DSC to calculate their T_g. According to our findings, the T_g of the lyophilisates was in the range of 55.5 – 58.1 °C (at 11% RH) and 34.6 – 48.4 °C (at 54% RH), with the lowest and highest T_g values observed in the SPI and WPI based systems, respectively. This suggests that all systems tested were found in the glassy state regardless of the RH. Despite this, the increase in RH accelerated the inactivation of bacterial cells due to elevated cellular metabolic activity and increased biochemical reaction rates during storage. Previous studies have reported a reciprocal relationship between T_g and probiotic cell inactivation rates (Hellebois et al., 2024), but we did not observe this in our case. For example, the WPI-based lyophilisates showed the lowest LGG stability during storage despite their very high T_g values. This indicates that other factors co-influenced the storage stability of probiotic lyophilisates.

In keeping with the findings of Guerrero Sanchez et al. (2022) who reported that the thermal history during the sublimation step and loss of the cellular integrity due to the damage of nucleic acids, proteins and peptidoglycans of *L. salivarius* during the lyophilisation govern its storage stability, the impaired survivability of LGG in the SPI and WPI systems is also associated with its lower cryo-resistance. In addition, the storage of probiotics at high dryness conditions (i.e., $\Delta T = T - T_g \ll 0$), may give rise to oxidative alterations of their membrane structural elements (e.g., lipids, nucleic acids etc.) reducing their cellular fluidity (Guerrero Sanchez et al., 2022). Although for freeze dried probiotics the reported the extent of the oxidative alteration of the membranes total PUFA content is generally low (< 2 – 5%), the presence of unsaturated lipids in the conveying wall material could accelerate the oxidative stress of the cells through the generation of ROS under low a_w conditions i.e., < 0.2. Despite the negligible residual lipid content in PPI and WPI, in the case of SPI-based lyophilisates, the presence of lipids rich in oleic, linoleic, and γ-linolenic acids (Cohen et al., 1987) could promote the formation of pro-oxidants – particularly at 37 °C – resulting in the

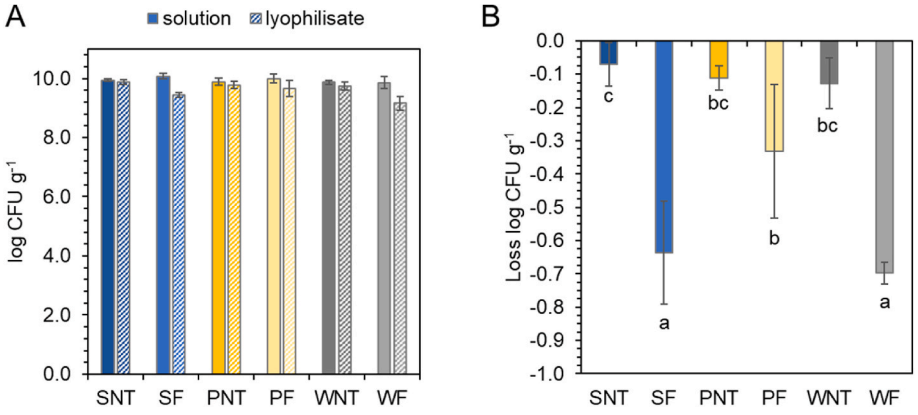

Fig. 8. Influence of protein composition (S = spirulina, P = pea, W = whey) and precursor treatment (NT = non-treated, F = fermented) on the total viable counts (A) and loss (B) of LGG cells during lyophilisation. $^{a\text{-}c}$Different letters denote a significant difference according to Tukey's post hoc means comparison test ($p < 0.05$).

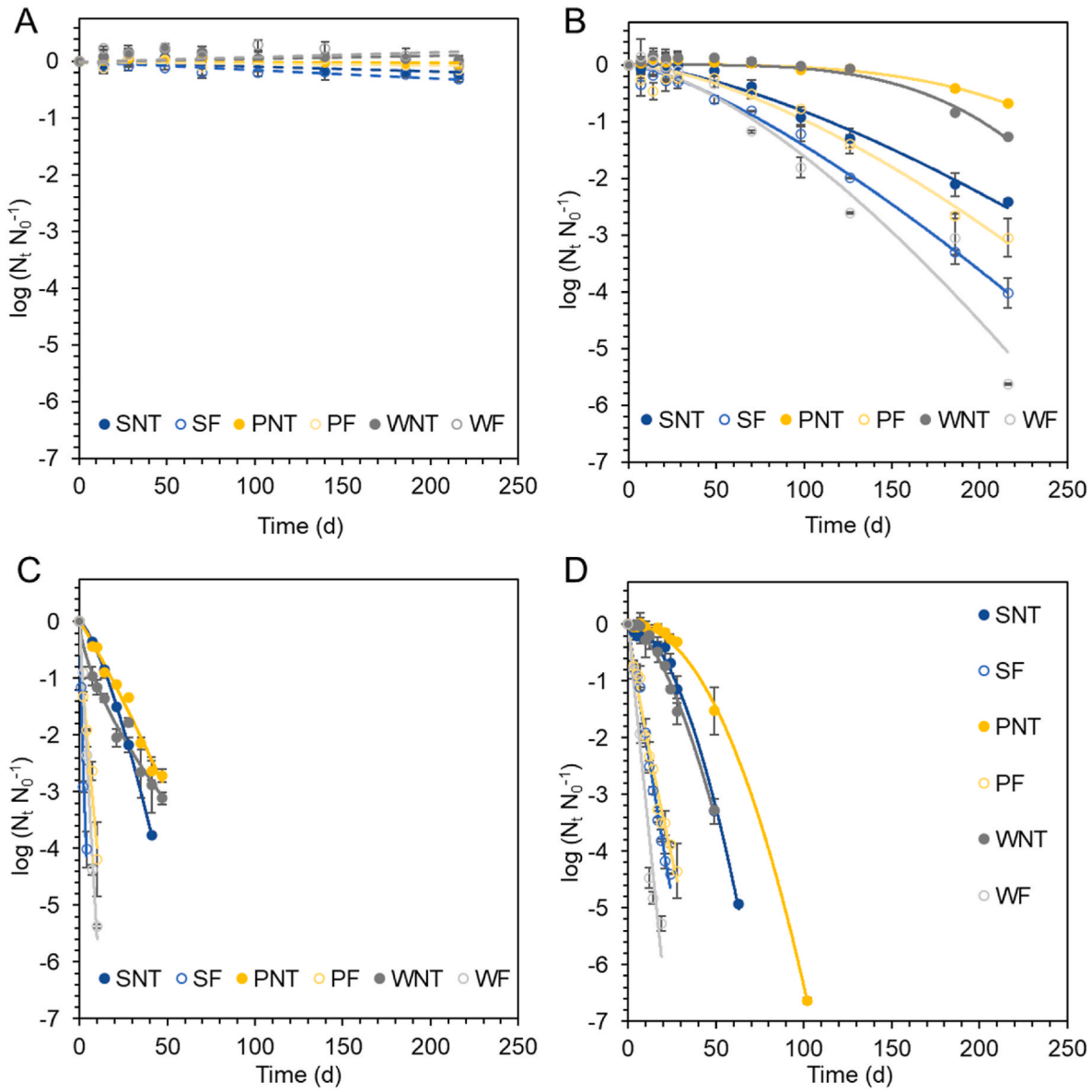

ig. 9. Influence of lyophilisate protein composition (S = spirulina, P = pea, W = whey) and precursor treatment (NT = non-treated, F = fermented) on the loss of viable LGG cells under controlled storage conditions (A: T = 4 °C, a_w = 0.11; B: T = 20 °C, a_w = 0.11; C: T = 20 °C, a_w = 0.54; D: T = 37 °C; a_w = 0.11). The modelling of the LGG cells inactivation kinetics was based on the Weibull model (Eq. (3)).

Table 5
Influence of lyophilisate protein composition (S = spirulina, P = pea, W = whey) and precursor pre-treatment (NT = non-treated, F = fermented) on the Weibull model (Eq. (3)) kinetic parameters α (in days) and β (dimensionless) of the inactivation of LGG cells as influenced by the storage conditions.

Sample	20 °C						37 °C		
	a_w 0.11			a_w 0.54			a_w 0.11		
	α	β	Adj. R^2	α	β	Adj. R^2	α	β	Adj. R^2
SNT	64.5 ± 16.3^{a}	1.5 ± 0.3^{a}	0.972	8.7 ± 0.5^{b}	1.4 ± 0.0^{c}	0.999	17.5 ± 3.5^{b}	1.9 ± 0.3^{b}	0.992
SF	41.4 ± 0.0^{a}	1.3 ± 0.0^{a}	0.987	0.2 ± 0.1^{a}	0.7 ± 0.1^{a}	0.951	2.0 ± 0.2^{a}	1.0 ± 0.0^{ab}	0.984
PNT	190 ± 1.0^{b}	3.5 ± 0.0^{b}	0.914	8.5 ± 0.0^{b}	1.1 ± 0.0^{bc}	0.975	28.5 ± 4.7^{c}	2.1 ± 0.3^{b}	0.997
PF	58.6 ± 10.5^{a}	1.5 ± 0.3^{a}	0.955	0.6 ± 0.3^{a}	0.8 ± 0.2^{ab}	0.972	1.8 ± 0.6^{a}	0.9 ± 0.1^{a}	0.971
WNT	162 ± 2.5^{b}	3.9 ± 0.3^{b}	0.939	2.3 ± 0.2^{b}	0.6 ± 0.0^{a}	0.944	14.1 ± 1.0^{b}	1.6 ± 0.1^{bc}	0.975
WF	41.4 ± 0.4^{a}	1.5 ± 0.0^{a}	0.939	0.7 ± 0.1^{a}	1.0 ± 0.1^{ab}	0.98	1.5 ± 0.2^{a}	1.0 ± 0.1^{ab}	0.941

[a-c]Different letters denote a significant difference according to Tukey's post hoc means comparison test ($p < 0.05$).

oxidation of the lipids in the LGG phospholipid wall particularly when stored at 37 °C.

To estimate the shelf-life (t_d) of the probiotic lyophilisates i.e., the time required for reaching the minimum total viable counts as established by the FAO/WHO i.e., 6 log CFU g^{-1}, Eq. (4) was used:

$$t_d = \alpha\left(-\ln\left(10^{-d}\right)^{1/\beta}\right) \quad (4)$$

where d is the number of decimal reductions, α (days) and β are the Weibull model kinetic parameters. As seen in Table 6, the estimated shelf of the probiotic lyophilisates stored at ambient temperature (11% RH) ranged from 151 to 348 days, which well above the reported values in the literature (Azizi et al., 2021). The increase in the storage temperature and RH was accompanied by dramatic shortening of the shelf life i.e., 10 to 77 and 4 to 61 days, respectively. On the other hand, the storage of the probiotic lyophilisates at chilling conditions resulted in a remarkably high shelf-life (>2 years, according to a rough estimation assuming first order LGG inactivation kinetics) confirming their suitability as nutraceuticals.

3.5.3. Viability of LGG throughout in vitro digestion

Monitoring the probiotic cells sublethality throughout gastrointestinal transit is crucial for understanding the biological performance of the conveying xero-template. As illustrated in Fig. 10, the non-encapsulated LGG cells experienced significant lethality during simulated gastric (2.75 log CFU g^{-1}) and intestinal (3.1 log CFU g^{-1}) digestion step in agreement with previous observations by Soukoulis et al. (2014). The embedment of the LGG cells into the protein enriched lyophilisates enhanced their ability to counteract the stressors associated with the gastrointestinal fluids, with cellular sublethality evident exclusively during the gastric processing step (0.62 – 2.76 log CFU g^{-1}). The implementation of the fermentation step prior to lyophilisation enhanced significantly ($p < 0.001$) the ability of the LGG to overcome, to some extent, the intragastric cellular stress (i.e., TVC losses were 2.46 and 1.37 log CFU g^{-1}), with the WF-based gastric chymes exerting the most pronounced effect. The ability of Lactobacilli to remove stress factors such as low pH and high bile salt utilising efflux systems such as proton pumps and multidrug resistance transporters (MDR) has been well documented (Lebeer et al., 2010). In addition, the upregulation of the *dlt* operon for the D-alanine esterification of teichoic acids to maintain the structural integrity of the LGG cell membrane is also known. As for the impact of the protein isolate type on the survivability of LGG cells in the gastric ambient, WPI offered the highest ($p < 0.01$) cellular protection compared to the SPI and PPI counterparts (i.e., TVC losses amounted to −2.32, −1.85 and −1.58 log CFU g^{-1}, respectively). Although the impact of the protein on the matrix disintegration has been closely associated with the sublethality of LGG cells in the gastric environment (Guerin et al., 2017), it was not possible to identify any clear correlation between the matrix disintegration and the LGG TVC at the end of the gastric processing. A possible explanation for the acid-stress alleviating capacity of the proteins may reside with their impact on the fermentation time (t_f = ca. 4 h, 1.5 h and 1.5 h for WPI, SPI and PPI, respectively). Hence, the LGG cells embedded in the WPI-based hydrogel matrices were longer adapted to acidic conditions, which enhanced their capacity to preserve their cell envelope integrity in the gastric fluids. Another explanation is the well-demonstrated bio-adhesion affinity of LGG cells surface biomolecules to WPI promoting their ability to withstand typical physicochemical stressors (Guerin et al., 2018).

Table 6
Influence of lyophilisate protein composition (S = spirulina, P = pea, W = whey) and precursor pre-treatment (NT = non-treated, F = fermented) on the shelf-life (TVC ≤6 log CFU g^{-1}) of the probiotic lyophilisates stored under different conditions calculated based on the Weibull model (Eqs. (3) and (4)).

Sample	a_w 0.11		a_w 0.54
	20 °C	37 °C	20 °C
SNT	290 ± 17.4	55 ± 0.4	42 ± 1.4
SF	210 ± 11.2	20 ± 0.5	4 ± 0.5
PNT	348 ± 7.4	77 ± 2.0	60 ± 1.7
PF	231 ± 15.5	20 ± 0.3	9 ± 1.4
WNT	282 ± 8.1	52 ± 0.7	61 ± 8.0
WF	151 ± 0.7	10 ± 0.5	5 ± 0.0

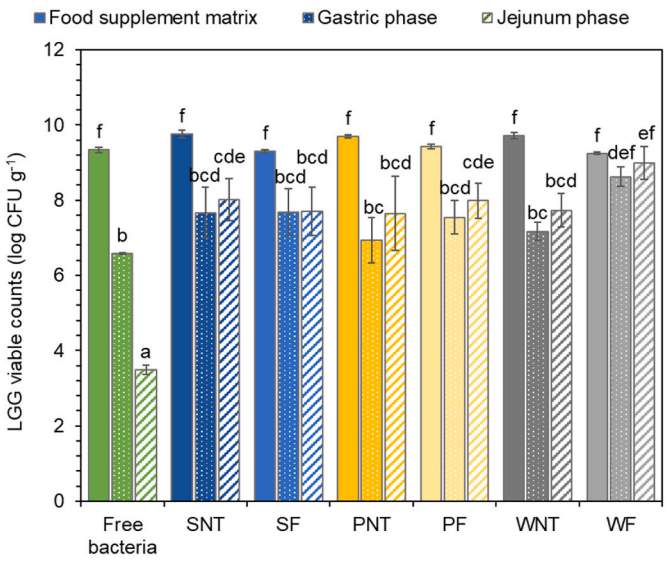

Fig. 10. Influence of lyophilisate protein composition (S = spirulina, P = pea, W = whey) and precursor treatment (NT = non-treated, F = fermented) on total viable LGG cell counts in the initial matrix and obtained gastric and intestinal chymes. [a-f]Different letters denote a significant difference according to Tukey's post hoc means comparison test ($p < 0.05$).

Contrary to the gastric processing, the exposure of LGG cells to intestinal fluids did not exhibit any significant effect on their viability ($p > 0.05$), with the TVC either remaining unaltered or even showing an increase at the end of the intestinal processing step (0.01 – 0.72 log CFU g^{-1}). Owing to their surface-active properties, bile salts can dissolve the lipids of the phospholipid cell wall and increase the permeability of the cell membrane damaging the intracellular proteins and DNA and facilitating the cytoplasmic leakage (Mendonça et al., 2022). Although *L. rhamnosus* GG is known for its sensitivity to high bile salt environments, the observed sublethality in the present study was negligible. The ability of probiotic bacteria to increase their bile salt resistance by upregulating the oligosaccharides degradation via the α-glycosidase, β-glycosidase and β-fucosidase has been demonstrated (Reyes-Gavilán et al., 2005). Hereby, this appears to be quite possible given the high content in hydrolysable oligosaccharides (M_w > 10 kDa) and sugars. Although the pre-fermentation step did not alter the resistance of LGG in the simulated jejunum environment, the protein type was more influential ($p < 0.05$). In the latter case, PPI and WPI promoted more effectively the growth of LGG cells in the intestinal chymes compared to SPI (i.e., 0.58, 0.46 and 0.18 log CFU g^{-1}, respectively). In line with our findings, Vargas et al. (2015) reported that WPI enhanced the bile salt resistance of yoghurt culture starters (i.e. *S. thermophilus* and *L. bulgaricus*) proportionally to its content. The observed alleviation of the bile salt mediated stress of LGG may be attributed to the ability of proteins to act as a barrier between the bile salt and phospholipid bilayer, thus preventing the increase in the LGG cell membrane permeability.

3.5.4. Adhesion of LGG cells to an in vitro human gut epithelium model

The ability of the carrier systems to promote the adhesion of the LGG cells to the gut mucosa was tested on a mucin-producing *in vitro* co-culture (Caco-2/HT-29) cell model (Fig. 11). As illustrated in the representative CLSM micrograph (Fig. 11 A1), a satisfactorily high number of non-injured LGG cells were adhered to the mucus-rich microdomains of the co-culture model. However, it should be noted that on some occasions, LGG cells suffering sublethal stress were also able to adhere to the mucus layer of the co-culture model (Fig. 11 A2).

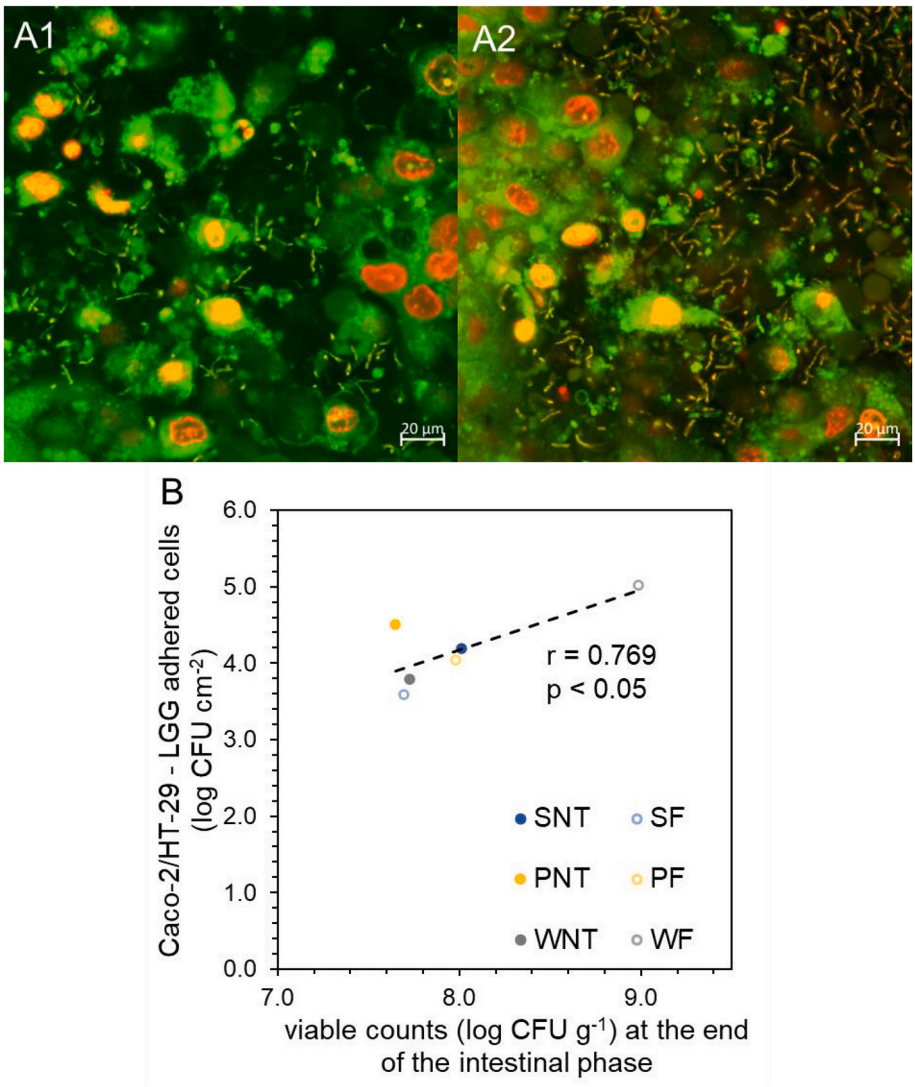

Fig. 11. (A): Representative CLSM micrographs (× 20) illustrating LGG cell adhesion to the mucus layer of a gut epithelium co-culture model, influenced by the pre-treatment of spirulina protein isolate-based precursors (A1: non-treated, A2: fermented), whereby green represents living bacteria and red dead bacteria. (B): Correlation between culturable LGG cell counts adhered to the mucosal layer of the gut epithelium co-culture model and total viable counts in the intestinal chymes, influenced by protein composition (S = spirulina, P = pea, W = whey) of the lyophilisates and pre-treatment of their precursors (NT = non-treated, F = fermented).

The number of cultivable LGG cells adhered ranged from 3.60 to 5.01 log CFU cm^{-2}. A positive correlation ($r = 0.769$, $p < 0.05$) between the LGG TVCs in the jejunum digesta and number of the living cells adhered to the mucosa of the co-culture model was found, implying the probabilistic character of the LGG cell adhesion properties (Fig. 11 B). The protein type was highly influential ($p < 0.001$) on the amount of LGG cell adhered to the mucosa of the co-culture model with the WPI and PPI to exhibit the highest muco-adhesion potential (4.40, 4.27 and 3.89 log CFU cm^{-2}, respectively). On the contrary, the implementation of the pre-fermentation step did not affect the LGG cells muco-adhesion performance (4.16 vs 4.21 log CFU cm^{-2} for NT and F). The establishment of probiotic cells in the gut microbiota ecosystem is largely modulated by their ability to adhere to the mucus layer of the gut epithelium and form a biofilm surrounded by extracellular polymeric substances (Lu et al., 2022). The adherence of probiotics to the intestinal epithelium is intricately linked to their hydrophobicity and auto-aggregation abilities depending on the number of the hydrophobic groups on the cells surface (Mendonça et al., 2022). In a recent study, Liu et al. (2022) demonstrated that co-culturing *L. plantarum* with 1% wt. of protein (whey, soy or Ilisha) improved its intestinal adhesion due to the enhancement of its cellular hydrophobicity and self-aggregation ability, which could explain the enhanced LGG intestinal adhesion in the case of the fermented WPI systems.

On the other hand, the interaction of bacterial cells with the food matrix components, in their intact or peptic cleaved form, may also affect their ability to adhere to the gut mucosa (Flach et al., 2018; Paone & Cani, 2020). In the present work, the proteolysis degree (OPA assay – data not shown) was well correlated with the number of the adhered LGG cells ($r = -0.987$, $p < 0.05$; Suppl. Fig. 2), which implies that the peptic cleavage of proteins diminishes their adhesive potential. In a previous study, Świątecka et al. (2010) demonstrated that pea protein isolate, in its either native or glycated form, enhanced the ability of *L. acidophilus* to adhere to the mucus layer of Caco-2/HT29 cells, an effect that was attributed to the ability of pea proteins to act as cell adhesion molecules. In another study, Deepika et al. (2011) reported that the composition (fat, sugar and pH) and storage time are likely to affect the adhesion of LGG to Caco-2 cells. Nonetheless, the literature data regarding the role of digested food macromolecules on the adhesion of probiotic cells is not well explored. Lastly, it is worth highlighting, that no significant effect of the storage period (fresh vs. 6 months stored under chilling conditions) on the LGG muco-adhesion properties was observed, confirming the preservation of the biological activity of the

lyophilisates over storage.

4. Conclusions

This study investigated the feasibility of utilising Spirulina platensis protein isolate (SPI) in creating protein-rich xero-templates that convey live *Lacticaseibacillus rhamnosus* GG (LGG) cells, drawing parallels with whey and pea protein isolates. Despite variations in microstructural features, SPI demonstrated a satisfactory capability to engraft live LGG cells into the wall material, akin to whey (WPI) and pea (PPI) protein isolate. The fermentation of the precursors impaired the ability of the LGG cells to withstand the physicochemical stressors associated with the lyophilisation process and storage conditions. In terms of preserving cell viability throughout freeze drying and subsequent storage, PPI-based xero-templates outperformed both SPI and WPI. It was postulated that several parameters such as the LGG adhesion affinity to proteins, the microstructure configuration of the engrafting xero-template and oxidative alterations of the cell membrane components – lipids, nucleic acids and proteins – potentially influenced the LGG viability. Although exposure to gastric conditions notably reduced the count of cultivable LGG cells, fermented lyophilisates enhanced LGG survivability, an effect attributed to the cells' adaptation to acidic environments. Furthermore, neither bile salts nor pancreases significantly affected LGG survival in intestinal chymes. A satisfactory LGG cell adhesion to the mucus layer of an in-vitro co-culture model of gut epithelium across all conditions was observed, with WPI and PPI appearing to promote the most the molecular interactions between LGG cells and the mucosa. In conclusion, this research affirmed the potential of SPI as a wall material for embedding and preserving the biological activity of LGG, with the results being particularly promising when compared to WPI. The findings from this work may contribute significantly to the development of effective and robust delivery systems for probiotics.

CRediT author statement

Jennyfer Fortuin: Conceptualisation, Investigation, Formal analysis, Writing Original Draft, Writing-Review-Editing, Funding Acquisition. Thierry Hellebois: Investigation, Formal analysis, Writing-Review & Editing. Marcus Iken: Writing-Review & Editing. Alexander Shaplov: Investigation, Formal analysis, Writing-Review & Editing. Vincenzo Fogliano: Conceptualisation, Writing-Review & Editing, Supervision (JF). Christos Soukoulis: Conceptualisation, Writing-Review & Editing, Supervision (JF), Project administration, Funding Acquisition.

Declaration of competing interest

The authors declare that they have no known competing financial interests or personal relationships that could have appeared to influence the work reported in this paper.

Data availability

Data will be made available on request.

Acknowledgements

The study was co-financed by the Luxembourg National Research Fund – FNR and PM-International AG (Project: ALGPRO, Project number: 15878670, Funding Scheme: Industrial Fellowships 2021-2).

Appendix A. Supplementary data

Supplementary data to this article can be found online at https://doi.org/10.1016/j.foodhyd.2023.109519.

References

Ahmed, J., & Kumar, V. (2022). Effect of high-pressure treatment on oscillatory rheology, particle size distribution and microstructure of microalgae Chlorella vulgaris and Arthrospira platensis. *Algal Research, 62*, 102617. https://doi.org/10.1016/j.algal.2021.102617.

Albalasmeh, A., Berhe, A., & Ghezzehei, T. (2013). A new method for rapid determination of carbohydrate and total carbon concentrations using UV spectrophotometry. *Carbohydrate Polymers, 97*, 253–261. https://doi.org/10.1016/j.carbpol.2013.04.072

Aschenbrenner, M., Först, P., & Kulozik, U. (2015). *Freeze-drying of probiotics*. https://doi.org/10.1201/b18807-15

Augustin, M. A., & Hemar, Y. (2009). Nano- and micro-structured assemblies for encapsulation of food ingredients. *Chemical Society Reviews, 38*(4), 902–912. https://doi.org/10.1039/B801739P

Azizi, S., Rezazadeh-Bari, M., Almasi, H., & Amiri, S. (2021). Microencapsulation of Lactobacillus rhamnosus using sesame protein isolate: Effect of encapsulation method and transglutaminase: Microencapsulated *L. rhamnosus* using sesame protein. *Food Bioscience, 41*. https://doi.org/10.1016/j.fbio.2021.101012. Scopus.

Benelhadj, S., Gharsallaoui, A., Degraeve, P., Attia, H., & Ghorbel, D. (2016). Effect of pH on the functional properties of Arthrospira (Spirulina) platensis protein isolate. *Food Chemistry, 194*, 1056–1063. https://doi.org/10.1016/j.foodchem.2015.08.133

van den Berg, C., & Bruin, S. (1981). Water activity and its estimation in food systems: Theoretical aspects. In *Water activity: Influences on food quality* (pp. 1–61). Elsevier. https://doi.org/10.1016/B978-0-12-591350-8.50007-3.

Bertsch, P., Böcker, L., Mathys, A., & Fischer, P. (2021). Proteins from microalgae for the stabilization of fluid interfaces, emulsions, and foams. *Trends in Food Science & Technology, 108*, 326–342. https://doi.org/10.1016/j.tifs.2020.12.014

Betz, M., García-González, C. A., Subrahmanyam, R. P., Smirnova, I., & Kulozik, U. (2012). Preparation of novel whey protein-based aerogels as drug carriers for life science applications. *The Journal of Supercritical Fluids, 72*, 111–119. https://doi.org/10.1016/j.supflu.2012.08.019

van Boekel, M. A. J. S. (2002). On the use of the Weibull model to describe thermal inactivation of microbial vegetative cells. *International Journal of Food Microbiology, 74*(1), 139–159. https://doi.org/10.1016/S0168-1605(01)00742-5

van Boekel, M. A. J. S. (2009). *Kinetic modeling of reactions in foods*. CRC Press.

Bortolini, D. G., Maciel, G. M., Fernandes, I. de A. A., Pedro, A. C., Rubio, F. T. V., Branco, I. G., & Haminiuk, C. W. I. (2022). Functional properties of bioactive compounds from Spirulina spp.: Current status and future trends. *Food Chemistry: Molecular Sciences, 5*, Article 100134. https://doi.org/10.1016/j.fochms.2022.100134

Boukhari, N., Doumandji, A., Sabrine Ait chaouche, F., & Ferradji, A. (2018). Effect of ultrasound treatment on protein content and functional properties of Spirulina powder grown in Algeria. *Mediterranean Journal of Nutrition and Metabolism, 11*(3), 235–249. https://doi.org/10.3233/MNM-180220

Brodkorb, A., Egger, L., Alminger, M., Alvito, P., Assunção, R., Ballance, S., … Recio, I. (2019). INFOGEST static in vitro simulation of gastrointestinal food digestion. *Nature Protocols, 14*(4), 991–1014. https://doi.org/10.1038/s41596-018-0119-1.

Broeckx, G., Vandenheuvel, D., Henkens, T., Kiekens, S., van den Broek, M. F. L., Lebeer, S., & Kiekens, F. (2017). Enhancing the viability of Lactobacillus rhamnosus GG after spray drying and during storage. *International Journal of Pharmaceutics, 534*(1–2), 35–41. https://doi.org/10.1016/j.ijpharm.2017.09.075. Scopus.

Buono, S., Langellotti, A. L., Martello, A., Rinna, F., & Fogliano, V. (2014). Functional ingredients from microalgae. *Food & Function, 5*(8), 1669–1685. https://doi.org/10.1039/C4FO00125G

Burgain, J., Corgneau, M., Scher, J., & Gaiani, C. (2015). Chapter 20—encapsulation of probiotics in milk protein microcapsules. In L. M. C. Sagis (Ed.), *Microencapsulation and microspheres for food applications* (pp. 391–406). Academic Press. http://www.sciencedirect.com/science/article/pii/B9780128003503000194.

Capela, P., Hay, T. K. C., & Shah, N. P. (2006). Effect of cryoprotectants, prebiotics and microencapsulation on survival of probiotic organisms in yoghurt and freeze-dried yoghurt. *Food Research International, 39*(2), 203–211. https://doi.org/10.1016/j.foodres.2005.07.007. Scopus.

Caporgno, M. P., & Mathys, A. (2018). Trends in microalgae incorporation into innovative food products with potential health benefits. *Frontiers in Nutrition, 5*. https://doi.org/10.3389/fnut.2018.00058

Capozzi, V., Arena, M. P., Russo, P., Spano, G., & Fiocco, D. (2016). Chapter 16 - stressors and food environment: Toward strategies to improve robustness and stress tolerance in probiotics. In R. R. Watson, & V. R. Preedy (Eds.), *Probiotics, prebiotics, and synbiotics* (pp. 245–256). Academic Press. http://www.sciencedirect.com/science/article/pii/B9780128021897000162.

Capozzi, V., Fiocco, D., & Spano, G. (2011). Responses of lactic acid bacteria to cold stress. In E. Tsakalidou, & K. Papadimitriou (Eds.), *Stress responses of lactic acid bacteria* (pp. 91–110). Springer US. https://doi.org/10.1007/978-0-387-92771-8_5.

Chaiklahan, R., Chirasuwan, N., Triratana, P., Loha, V., Tia, S., & Bunnag, B. (2013). Polysaccharide extraction from Spirulina sp. and its antioxidant capacity. *International Journal of Biological Macromolecules, 58*, 73–78. https://doi.org/10.1016/j.ijbiomac.2013.03.046

Chen, Y., Chen, J., Chang, C., Chen, J., Cao, F., Zhao, J., Zheng, Y., & Zhu, J. (2019). Physicochemical and functional properties of proteins extracted from three microalgal species. *Food Hydrocolloids, 96*, 510–517. https://doi.org/10.1016/j.foodhyd.2019.05.025

Cohen, Z., Vonshak, A., & Richmond, A. (1987). Fatty acid composition of Spirulina strains grown under various environmental conditions. *Phytochemistry, 26*(8), 2255–2258. https://doi.org/10.1016/S0031-9422(00)84694-4

Cui, S., Hang, F., Liu, X., Xu, Z., Liu, Z., Zhao, J., Zhang, H., & Chen, W. (2018). Effect of acids produced from carbohydrate metabolism in cryoprotectants on the viability of freeze-dried Lactobacillus and prediction of optimal initial cell concentration. *Journal of Bioscience and Bioengineering, 125*(5), 513–518. https://doi.org/10.1016/j.jbiosc.2017.12.009. Scopus.

Deepika, G., Rastall, R. A., & Charalampopoulos, D. (2011). Effect of food models and low-temperature storage on the adhesion of Lactobacillus rhamnosus GG to caco-2 cells. *Journal of Agricultural and Food Chemistry, 59*(16), 8661–8666. https://doi.org/10.1021/jf2018287

Dos Santos Morais, R., Gaiani, C., Borges, F., & Burgain, J. (2022). Interactions microbe-matrix in dairy products. In P. L. H. McSweeney, & J. P. McNamara (Eds.), *Encyclopedia of dairy sciences* (3rd ed., pp. 133–143). Academic Press. https://doi.org/10.1016/B978-0-08-100596-5.23004-7.

Flach, J., van der Waal, M. B., van den Nieuwboer, M., Claassen, E., & Larsen, O. F. A. (2018). The underexposed role of food matrices in probiotic products: Reviewing the relationship between carrier matrices and product parameters. *Critical Reviews in Food Science and Nutrition, 58*(15), 2570–2584. https://doi.org/10.1080/10408398.2017.1334624

Frost, & Sullivan. (2023). *Growth opportunities in alternative protein ingredients for human nutrition*. https://store.frost.com/growth-opportunities-in-alternative-protein-ingredients-for-human-nutrition.html.

Garcia-Brand, A. J., Quezada, V., Gonzalez-Melo, C., Bolaños-Barbosa, A. D., Cruz, J. C., & Reyes, L. H. (2022). Novel developments on stimuli-responsive probiotic encapsulates: From smart hydrogels to nanostructured platforms. *Fermentation, 8*(3), 117. https://doi.org/10.3390/fermentation8030117

Grossmann, L., Hinrichs, J., & Weiss, J. (2020). Cultivation and downstream processing of microalgae and cyanobacteria to generate protein-based technofunctional food ingredients. *Critical Reviews in Food Science and Nutrition, 60*(17), 2961–2989. https://doi.org/10.1080/10408398.2019.1672137

Guerin, J., Burgain, J., Borges, F., Bhandari, B., Desobry, S., Scher, J., & Gaiani, C. (2017). Use of imaging techniques to identify efficient controlled release systems of *Lactobacillus rhamnosus* GG during *in vitro* digestion. *Food & Function, 8*(4), 4. https://doi.org/10.1039/C6FO01737A

Guerin, J., Burgain, J., Francius, G., El-Kirat-Chatel, S., Beaussart, A., Scher, J., & Gaiani, C. (2018). Adhesion of *Lactobacillus rhamnosus* GG surface biomolecules to milk proteins. *Food Hydrocolloids, 82*, 296–303. https://doi.org/10.1016/j.foodhyd.2018.04.016

Guerrero Sanchez, M., Passot, S., Campoy, S., Olivares, M., & Fonseca, F. (2022). Effect of protective agents on the storage stability of freeze-dried Ligilactobacillus salivarius CECT5713. *Applied Microbiology and Biotechnology, 106*(21), 7235–7249. https://doi.org/10.1007/s00253-022-12201-9

Gu, Q., Yin, Y., Yan, X., Liu, X., Liu, F., & McClements, D. J. (2022). Encapsulation of multiple probiotics, synbiotics, or nutrabiotics for improved health effects: A review. *Advances in Colloid and Interface Science, 309*, Article 102781. https://doi.org/10.1016/j.cis.2022.102781

Hansen, L., Bu, F., & Ismail, B. P. (2022). Structure-Function guided extraction and scale-up of pea protein isolate production. *Foods, 11*(23), 3773. https://doi.org/10.3390/foods11233773

Hartmann, M., & Palzer, S. (2011). Caking of amorphous powders—material aspects, modelling and applications. *Powder Technology, 206*(1–2), 112–121. https://doi.org/10.1016/j.powtec.2010.04.014

Hellebois, T., Canuel, R., Addiego, F., Audinot, J.-N., Gaiani, C., Shaplov, A. S., & Soukoulis, C. (2023). Milk protein-based cryogel monoliths as novel encapsulants of probiotic bacteria. Part I: Microstructural, physicochemical, and mechanical characterisation. *Food Hydrocolloids, 140*. https://doi.org/10.1016/j.foodhyd.2023.108641. Scopus.

Hellebois, T., Canuel, R., Leclercq, C. C., Gaiani, C., & Soukoulis, C. (2024). Milk protein-based cryogel monoliths as novel encapsulants of probiotic bacteria. Part II: *Lacticaseibacillus rhamnosus* GG storage stability and bioactivity under *in vitro* digestion. *Food Hydrocolloids, 146*, Article 109173. https://doi.org/10.1016/j.foodhyd.2023.109173 (in press).

Hill, C., Guarner, F., Reid, G., Gibson, G. R., Merenstein, D. J., Pot, B., Morelli, L., Canani, R. B., Flint, H. J., Salminen, S., Calder, P. C., & Sanders, M. E. (2014). The International Scientific Association for Probiotics and Prebiotics consensus statement on the scope and appropriate use of the term probiotic. *Nature Reviews Gastroenterology & Hepatology, 11*(8), 506–514. https://doi.org/10.1038/nrgastro.2014.66

Hlaing, M. M., Wood, B. R., McNaughton, D., Ying, D., Dumsday, G., & Augustin, M. A. (2017). Effect of drying methods on protein and DNA conformation changes in *Lactobacillus rhamnosus* GG cells by fourier transform infrared spectroscopy. *Journal of Agricultural and Food Chemistry, 65*(8), 1724–1731. https://doi.org/10.1021/acs.jafc.6b05508

Hoobin, P., Burgar, I., Zhu, S., Ying, D., Sanguansri, L., & Augustin, M. A. (2013). Water sorption properties, molecular mobility and probiotic survival in freeze dried protein-carbohydrate matrices. *Food & Function, 4*(9), 1376–1386. https://doi.org/10.1039/c3fo60112a. Scopus.

Jackson, M., & Mantsch, H. H. (1995). The use and misuse of FTIR spectroscopy in the determination of protein structure. *30*(2), 95–120.

Kang, Y.-R., Lee, Y.-K., Kim, Y. J., & Chang, Y. H. (2019). Characterization and storage stability of chlorophylls microencapsulated in different combination of gum Arabic and maltodextrin. *Food Chemistry, 272*, 337–346. https://doi.org/10.1016/j.foodchem.2018.08.063

Kieps, J., & Dembczyński, R. (2022). Current trends in the production of probiotic formulations. *Foods, 11*(15), 2330. https://doi.org/10.3390/foods11152330

Kim, W., Wang, Y., Vongsvivut, J., Ye, Q., & Selomulya, C. (2023). On surface composition and stability of β-carotene microcapsules comprising pea/whey protein complexes by synchrotron-FTIR microspectroscopy. *Food Chemistry, 426*, Article 136565. https://doi.org/10.1016/j.foodchem.2023.136565

Kurtmann, L., Carlsen, C. U., Skibsted, L. H., & Risbo, J. (2009). Water activity-temperature state diagrams of freeze-dried *Lactobacillus acidophilus* (La-5): Influence of physical state on bacterial survival during storage. *Biotechnology Progress, 25*(1), 265–270. https://doi.org/10.1002/btpr.96

Lafarga, T., Fernández-Sevilla, J. M., González-López, C., & Acién-Fernández, F. G. (2020). Spirulina for the food and functional food industries. *Food Research International, 137*, Article 109356. https://doi.org/10.1016/j.foodres.2020.109356

Lebeer, S., Vanderleyden, J., & Keersmaecker, S. D. (2010). Adaptation factors of the probiotic *Lactobacillus rhamnosus* GG. *Beneficial Microbes*. https://doi.org/10.3920/BM2010.0032

Liu, G., Chu, M., Nie, S., Xu, X., & Ren, J. (2022). Effects of Ilisha elongata protein, soy protein and whey protein on growth characteristics and adhesion of probiotics. *Current Research in Food Science, 5*, 2125–2134. https://doi.org/10.1016/j.crfs.2022.10.024

Loveday, S. M. (2022). Protein digestion and absorption: The influence of food processing. *Nutrition Research Reviews*, 1–16. https://doi.org/10.1017/S0954422422000245

Lu, Y., Han, S., Zhang, S., Wang, K., Lv, L., McClements, D. J., Xiao, H., Berglund, B., Yao, M., & Li, L. (2022). The role of probiotic exopolysaccharides in adhesion to mucin in different gastrointestinal conditions. *Current Research in Food Science, 5*, 581–589. https://doi.org/10.1016/j.crfs.2022.02.015

Meireles Mafaldo, Í., de Medeiros, V. P. B., da Costa, W. K. A., da Costa Sassi, C. F., da Costa Lima, M., de Souza, E. L., Eduardo Barão, C., Colombo Pimentel, T., & Magnani, M. (2022). Survival during long-term storage, membrane integrity, and ultrastructural aspects of Lactobacillus acidophilus 05 and Lacticaseibacillus casei 01 freeze-dried with freshwater microalgae biomasses. *Food Research International, 159*, Article 111620. https://doi.org/10.1016/j.foodres.2022.111620

Mendonça, A. A., Pinto-Neto, W. de P., da Paixão, G. A., Santos, D. da S., De Morais, M. A., & De Souza, R. B. (2022). Journey of the probiotic bacteria: Survival of the fittest. *Microorganisms, 11*(1), 95. https://doi.org/10.3390/microorganisms11010095

Moll, P., Salminen, H., Seitz, O., Schmitt, C., & Weiss, J. (2022). Characterization of soluble and insoluble fractions obtained from a commercial pea protein isolate. *Journal of Dispersion Science and Technology*, 1–12. https://doi.org/10.1080/01932691.2022.2093214.

Moreira, C., Machado, L., Silva, M., Nunes, R., Pereira, R. N., Rocha, C. M. R., Geada, P., & Teixeira, J. A. (2023). Algal proteins. In *Reference module in food science*. Elsevier. https://doi.org/10.1016/B978-0-12-823960-5.00090-1.

Nicolai, T. (2019). Gelation of food protein-protein mixtures. *Advances in Colloid and Interface Science, 270*, 147–164. https://doi.org/10.1016/j.cis.2019.06.006

Paone, P., & Cani, P. D. (2020). Mucus barrier, mucins and gut microbiota: The expected slimy partners? *Gut, 69*(12), 2232–2243. https://doi.org/10.1136/gutjnl-2020-322260

Passot, S., Cenard, S., Douania, I., Tréléa, I. C., & Fonseca, F. (2012). Critical water activity and amorphous state for optimal preservation of lyophilised lactic acid bacteria. *Food Chemistry, 132*(4), 1699–1705. https://doi.org/10.1016/j.foodchem.2011.06.012

Paula, S. F. A., Chagas, B. M. E., Pereira, M. I. B., Rangel, A. H. N., Sassi, C. F. C., Borba, L. H. F., Santos, E. S., Asevedo, E. A., Câmara, F. R. A., & Araújo, R. M. (2022). Pyrolysis-GCMS of Spirulina platensis: Evaluation of biomasses cultivated under autotrophic and mixotrophic conditions. *PLoS One, 17*(10), Article e0276317. https://doi.org/10.1371/journal.pone.0276317

Pehkonen, K. S., Roos, Y. H., Miao, S., Ross, R. P., & Stanton, C. (2008). State transitions and physicochemical aspects of cryoprotection and stabilization in freeze-drying of *Lactobacillus rhamnosus* GG (LGG). *Journal of Applied Microbiology, 104*(6), 1732–1743. https://doi.org/10.1111/j.1365-2672.2007.03719.x. Scopus.

Pelegrine, D. H. G., & Gasparetto, C. A. (2005). Whey proteins solubility as function of temperature and pH. *LWT - Food Science and Technology, 38*(1), 77–80. https://doi.org/10.1016/j.lwt.2004.03.013

Pinho, L. S., de Lima, P. M., de Sá, S. H. G., Chen, D., Campanella, O. H., da Costa Rodrigues, C. E., & Favaro-Trindade, C. S. (2022). Encapsulation of rich-carotenoids extract from guaraná (paullinia cupana) byproduct by a combination of spray drying and spray chilling. *Foods, 11*(17), 17. https://doi.org/10.3390/foods11172557

Reyes-Gavilán, C. G., de los, Ruas-Madiedo, P., Noriega, L., Cuevas, I., Sánchez, B., & Margolles, A. (2005). Effect of acquired resistance to bile salts on enzymatic activities involved in the utilisation of carbohydrates by bifidobacteria. An overview. *Le Lait, 85*(1–2), 113–123. https://doi.org/10.1051/lait:2004028

Ricós-Muñoz, N., Rivas Soler, A., Castagnini, J. M., Moral, R., Barba, F. J., & Pina-Pérez, M. C. (2023). Improvement of the probiotic growth-stimulating capacity of microalgae extracts by pulsed electric fields treatment. *Innovative Food Science & Emerging Technologies, 83*, Article 103256. https://doi.org/10.1016/j.ifset.2022.103256

Roy, I., & Gupta, M. N. (2004). Freeze-drying of proteins: Some emerging concerns. *Biotechnology and Applied Biochemistry, 39*(2), 165–177. https://doi.org/10.1042/BA20030133

Saavedra-Leos, Z., Leyva-Porras, C., Araujo-Díaz, S. B., Toxqui-Terán, A., & Borrás-Enríquez, A. J. (2015). Technological application of maltodextrins according to the degree of polymerization. *Molecules (Basel, Switzerland), 20*(12), 21067–21081. https://doi.org/10.3390/molecules201219746

Safi, C., Charton, M., Pignolet, O., Silvestre, F., Vaca-Garcia, C., & Pontalier, P.-Y. (2013). Influence of microalgae cell wall characteristics on protein extractability and determination of nitrogen-to-protein conversion factors. *Journal of Applied Phycology, 25*(2), 523–529. https://doi.org/10.1007/s10811-012-9886-1

Şanlier, N., Gökcen, B. B., & Sezgin, A. C. (2019). Health benefits of fermented foods. *Critical Reviews in Food Science and Nutrition, 59*(3), 506–527. https://doi.org/10.1080/10408398.2017.1383355

Schwab, C., Vogel, R., & Gänzle, M. G. (2007). Influence of oligosaccharides on the viability and membrane properties of Lactobacillus reuteri TMW1.106 during freeze-drying. *Cryobiology, 55*(2), 108–114. https://doi.org/10.1016/j.cryobiol.2007.06.004

Seifert, A., Kashi, Y., & Livney, Y. D. (2019). Delivery to the gut microbiota: A rapidly proliferating research field. *Advances in Colloid and Interface Science, 274*, Article 102038. https://doi.org/10.1016/j.cis.2019.102038

Shkolnikov Lozober, H., Okun, Z., & Shpigelman, A. (2021). The impact of high-pressure homogenization on thermal gelation of Arthrospira platensis (Spirulina) protein concentrate. *Innovative Food Science & Emerging Technologies, 74*, Article 102857. https://doi.org/10.1016/j.ifset.2021.102857

Soni, R. A., Sudhakar, K., & Rana, R. S. (2017). Spirulina – from growth to nutritional product: A review. *Trends in Food Science & Technology, 69*, 157–171. https://doi.org/10.1016/j.tifs.2017.09.010

Soukoulis, C., Yonekura, L., Gan, H.-H., Behboudi-Jobbehdar, S., Parmenter, C., & Fisk, I. (2014). Probiotic edible films as a new strategy for developing functional bakery products: The case of pan bread. *Food Hydrocolloids, 39*, 231–242. https://doi.org/10.1016/j.foodhyd.2014.01.023

Świątecka, D., Małgorzata, I., Aleksander, Ś., Henryk, K., & Elżbieta, K. (2010). The impact of glycated pea proteins on bacterial adhesion. *Food Research International, 43*(6), 1566–1576. https://doi.org/10.1016/j.foodres.2010.03.003

Vargas, L. A., Olson, D. W., & Aryana, K. J. (2015). Whey protein isolate improves acid and bile tolerances of Streptococcus thermophilus ST-M5 and Lactobacillus delbrueckii ssp. Bulgaricus LB-12. *Journal of Dairy Science, 98*(4), 2215–2221. https://doi.org/10.3168/jds.2014-8869

Wang, Y., Corrieu, G., & Béal, C. (2005). Fermentation pH and temperature influence the cryotolerance of Lactobacillus acidophilus RD758. *Journal of Dairy Science, 88*(1), 21–29. https://doi.org/10.3168/jds.S0022-0302(05)72658-8

Wang, Y.-C., Yu, R.-C., & Chou, C.-C. (2004). Viability of lactic acid bacteria and bifidobacteria in fermented soymilk after drying, subsequent rehydration and storage. *International Journal of Food Microbiology, 93*(2), 209–217. https://doi.org/10.1016/j.ijfoodmicro.2003.12.001. Scopus.

Yao, M., Xie, J., Du, H., McClements, D. J., Xiao, H., & Li, L. (2020). Progress in microencapsulation of probiotics: A review. *Comprehensive Reviews in Food Science and Food Safety, 19*(2), 857–874. https://doi.org/10.1111/1541-4337.12532

Ye, A. (2021). Gastric colloidal behaviour of milk protein as a tool for manipulating nutrient digestion in dairy products and protein emulsions. *Food Hydrocolloids, 115*, Article 106599. https://doi.org/10.1016/j.foodhyd.2021.106599

Ying, D. Y., Phoon, M. C., Sanguansri, L., Weerakkody, R., Burgar, I., & Augustin, M. A. (2010). Microencapsulated *Lactobacillus rhamnosus* GG powders: Relationship of powder physical properties to probiotic survival during storage. *Journal of Food Science, 75*(9), E588–E595. https://doi.org/10.1111/j.1750-3841.2010.01838.x. Scopus.

Ying, D., Sun, J., Sanguansri, L., Weerakkody, R., & Augustin, M. A. (2012). Enhanced survival of spray-dried microencapsulated *Lactobacillus rhamnosus* GG in the presence of glucose. *Journal of Food Engineering, 109*(3), 597–602. https://doi.org/10.1016/j.jfoodeng.2011.10.017

Yonekura, L., Sun, H., Soukoulis, C., & Fisk, I. (2014). Microencapsulation of Lactobacillus acidophilus NCIMB 701748 in matrices containing soluble fibre by spray drying: Technological characterization, storage stability and survival after *in vitro* digestion. *Journal of Functional Foods, 6*, 205–214. https://doi.org/10.1016/j.jff.2013.10.008

Yuan, Y., Yin, M., Chen, L., Liu, F., Chen, M., & Zhong, F. (2022). Effect of calcium ions on the freeze-drying survival of probiotic encapsulated in sodium alginate. *Food Hydrocolloids, 130*, Article 107668. https://doi.org/10.1016/j.foodhyd.2022.107668